3708-15-T/5178-8-T

ANALOG COMPUTATION OF TIME-VARYING POWER SPECTRA OF SEISMIC WAVES

VERNON L. LARROWE
RAYMOND E. CRABTREE

ANALOG COMPUTER LABORATORY
Institute of Science and Technology
THE UNIVERSITY OF MICHIGAN

April 1963

Contracts AF 49(638)-911; AF 49(638)-1170

NOTICES

Sponsorship. The work reported herein was conducted by the Institute of Science and Technology for the U. S. Air Force under Contracts AF 49(638)-911 and AF 49(638)-1170. Contracts and grants to The University of Michigan for the support of sponsored research by the Institute of Science and Technology are administered through the Office of the Vice-President for Research.

ASTIA availability. Qualified requesters may obtain copies of this document from:

Armed Services Technical Information Agency
Arlington Hall Station
Arlington 12, Virginia

Final Disposition. After this document has served its purpose, it may be destroyed. Please do not return it to the Institute of Science and Technology.

FOREWORD

The Acoustics and Seismics Laboratory of the Institute of Science and Technology at The University of Michigan has been conducting research on seismic wave propagation during the past two years under Air Force Contract AF 49(638)-911. The collections of a considerable number of magnetic-tape recordings of seismic events under this and other contracts have presented a problem of data analysis. The same problem, only on a much larger scale, is currently being encountered in the VELA UNIFORM program.

It was thought that the use of analog and digital computers could conceivably speed up and improve the analyses of seismic recordings. Hence, the assistance of the Analog Computer Laboratory at the Institute of Science and Technology was enlisted to determine the feasibility of using analog-computer techniques to solve many of the problems.

This report covers the theoretical background and the results and conclusions that have been reached to date on the use of analog-computer techniques for the analysis of seismic data at The University of Michigan.

The authors would like to acknowledge the assistance of the following members of the Acoustics and Seismics Laboratory: J. M. DeNoyer, P. L. Jackson, J. A. Prout, and D. E. Willis.

CONTENTS

FIGURES

SYMBOLS

t = Time

$f(t)$ = Time function

A_o, A_n, B_n = Fourier series coefficients

ω_1 = Fundamental angular frequency $\left(\frac{2\pi}{T}\right)$

f_1 = Fundamental frequency $\left(\frac{1}{T}\right)$

T = Period of periodic wave, or length of portion of f(t) being analyzed

$P(t)$ = Instantaneous power dissipation in 1-ohm resistor

P_{av} = Average power

$P(n)$ = Power in the n-th trigonometric Fourier component

$a(\omega)$, $b(\omega)$ = Fourier integral coefficients

W = Total energy dissipated across a 1-ohm resistor with applied voltage f(t)

$W(\omega_j)$ = Energy contained in all frequencies from 0 to ω_j

$W_d(\omega)$ = Energy-density spectrum (function of ω) (energy/(rad/sec)-bandwidth at ω)

ω_c = Carrier frequency

ω_m = Modulating frequency

$W_d(\omega, t_o)$ = Time-varying energy-density spectrum at time t_o

$p(\omega, t_o)$ = Double-sided power density spectrum at time t_o

$P(\omega, t_o)$ = One-sided power density spectrum at time t_o; $2\left[p(\omega, t_o)\right] = P(\omega, t_o)$

$G(\omega - \omega_o)$ = Filter transfer function

$p(n)$ = Power in the n-th exponentially-defined Fourier component; $P(n) = 2p(n)$

$p(n\omega_1)$ = Power density in watts per radian per second, at the value of ω which is equal to $n\omega_1$

$Q(t - t_o)$ = Weighting function

$f_1(t - t_o)$ = Time aperture or window; $Q(t - t_o) = f_1^2(t - t_o)$

$p(\omega)$ = Power density in watts per radian per second at ω

K = Normalizing factor

$F(\omega)$ = Fourier transform of f(t)

$\bar{F}(\omega)$ = Complex conjugate of $F(\omega)$

F_I = Interrogation frequency used in analog-computer circuit

$h(t)$ = Response of an electrical network to a unit impulse

E_n = Analog-computer voltage

α = Reciprocal of first-order filter time constant

$p_\alpha(\omega)$ = Exponentially mapped past (e.m.p.) power spectrum

ω_i = Interrogation angular frequency used in analog-computer circuit, ($\omega_i \approx 2\pi F_i$)

ω_o = Frequency coordinate of time-varying power spectrum $p(\omega_o, t_o)$

t_o = Time coordinate of time-varying power spectrum $p(\omega_o, t_o)$

ANALOG COMPUTATION OF TIME-VARYING POWER SPECTRA OF SEISMIC WAVES

ABSTRACT

An analog computing technique for measuring time-varying power spectra of seismic signals has been developed. The signal to be analyzed is recorded on a magnetic-tape loop so that it may be played back repeatedly, and the analog computing equipment, connected to the output of the tape-playback apparatus, measures as a function of time the power level at a different specific frequency for each passage of the tape.

The concept of a time-varying spectrum is developed and the theory of the analysis method used is derived. It is shown that in measuring time-varying power spectra, there is a theoretical relationship between the time resolution and frequency resolution such that any adjustment which gives an improvement in one results in a degradation of the other. This conflict is not caused by equipment limitations, but instead is a result of theoretical relations between the time and frequency domains.

A plot of the energy- or power-density spectrum of a seismic wave is not smooth, but instead shows a number of sharply defined peaks. It was found experimentally that a filter bandwidth of 2 1/2% for the analyzing apparatus gave satisfactory frequency resolution without seriously degrading time resolution when magnetic-tape seismograms were analyzed.

It is concluded that measuring methods based on the use of filters are theoretically equivalent to methods using weighted Fourier analysis, and that the choice of a method to be used should be based primarily upon equipment requirements. The analog-computer setup makes a very flexible tool for developing methods of power-spectra measurements, although more specialized apparatus would probably be more satisfactory after an optimum method has been found.

There is a possibility for considerable improvement in the measuring techniques, and it is recommended that research directed toward optimizing the analysis of seismic waves be continued.

1
INTRODUCTION

This report describes analog computing methods which were employed in measuring the time-varying frequency spectra of seismic waves. Formal analytical methods, using the Fourier series or Fourier integral formulas, are not directly applicable, since these methods yield sinusoids of constant amplitude. In fact, a sinusoid whose amplitude or envelope varies as a function of time does not really represent a single frequency, but instead is made up of a carrier frequency plus sidebands. If time variations in amplitude of a frequency component are permitted, the value of frequency cannot be specified exactly, or if the exact frequency of a component is specified, then variations in its amplitude are impossible.

The concept of a signal made up of amplitude-modulated frequency components is not difficult to understand. An example is the group of all of the radio signals in the broadcast band. These consist of amplitude-modulated carrier frequencies, spaced 10 kc apart and occupying the frequency band from 550 to 1500 kc. A broadcast radio receiver serves as an "analyzer" in that it selects any desired frequency and through a "detection" process produces a signal corresponding to the time variation of the frequency component's amplitude.

The various frequency components of seismic surface waves propagate at different velocities and, in the case of body waves, by different paths. Consequently the arrival times for the different phases at a recording point which is far removed from the source of the initial disturbance will occur at different times, and portions of the wave train will be dispersed.

In analyzing the seismogram, it is important to determine accurately the time of arrival and duration of each major frequency component. Any frequency-analysis method employed should be capable of accurately measuring the time variations of a specific frequency component, but should at the same time be capable of separating the various frequency components. These two requirements conflict, since improvement of performance on one of them results in degradation in performance on the other. The following section of this report discusses the basic problem and its solution in more detail.

2
THEORY

2.1. CONVENTIONAL SPECTRAL ANALYSIS

2.1.1. FOURIER SERIES. If a seismic signal is defined for the interval $0 \leq t \leq T$, it can be synthesized within this interval from a Fourier trigonometric series. The terms of the Fourier series are harmonically related. If the length of the signal being analyzed is T seconds, the lowest or fundamental frequency of the Fourier series expansion would be $f_1 = \frac{1}{T}$ cps. All other frequencies of the Fourier terms would then be integral multiples of this fundamental frequency. Thus, within the interval $0 \leq t \leq T$, the signal would be represented by a series of the form

$$f(t) = \frac{A_o}{2} + \sum_{n=1}^{\infty} (A_n \cos n\omega_1 t + B_n \sin n\omega_1 t) \tag{1}$$

where $\omega_1 = 2\pi f_1 = 2\pi/T$ (radians per second) and the coefficients are defined as follows:

$$A_o = \frac{2}{T} \int_0^T f(t)\, dt \tag{2}$$

$$A_n = \frac{2}{T}\int_0^T f(t) \cos n\omega_1 t\,dt \tag{3}$$

$$B_n = \frac{2}{T}\int_0^T f(t) \sin n\omega_1 t\,dt \tag{4}$$

If the Fourier series for a function f(t) is computed and the terms are added as specified by Equation 1, the result is f(t) for $0 \leq t \leq T$, but the function is periodic. That is, $f(nT + t) = f(t)$ for $(n = 0, \pm1, \pm2, \ldots)$. Thus, the function obtained from the Fourier series does not exactly correspond to the original function, for which $f(nT + t) = 0$ for $(n = \pm1, \pm2, \pm3, \ldots)$.

Plots of A_n vs. n, and B_n vs. n result in "line" spectra, which have values for integral values of n only. Plots of this type are shown in Figure 1.

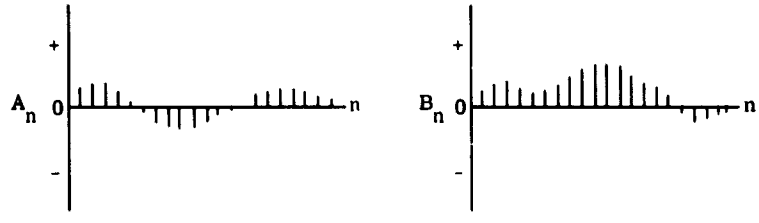

FIGURE 1. EXAMPLES OF "LINE" FREQUENCY SPECTRA

If f(t) is a voltage which is applied across a 1-ohm resistive load, the instantaneous power dissipated in the load at any time t is given by

$$P(t) = f^2(t) \tag{5}$$

and the average power, in the interval $0 \leq t \leq T$, is given by

$$P_{av} = \frac{1}{T}\int_0^T [f(t)]^2\,dt$$

Since the average power produced in the load by a sinusoidal voltage of amplitude A is $A^2/2$, the average power level of the n-th harmonic of the Fourier series is given by

$$P(n) = \frac{A_n^2}{2} + \frac{B_n^2}{2} \tag{6}$$

The sum of the average power levels of the Fourier components is equal to the average power in f(t) in the interval from $0 \leq t \leq T$.

Thus

$$\sum_{n=0}^{\infty} \frac{A_n^2 + B_n^2}{2} = \sum_{n=0}^{\infty} P(n) = \frac{1}{T}\int_0^T [f(t)]^2 dt \qquad (7)$$

A power spectrum for f(t) may be obtained by plotting P(n) as a function of n. A sketch of a typical plot is shown in Figure 2.

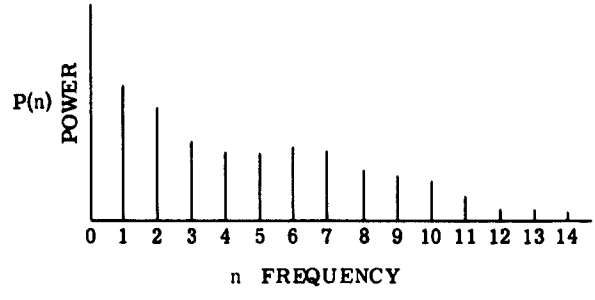

FIGURE 2. EXAMPLE OF A LINE POWER SPECTRUM

Note that the function P(n) has values only for integral values of n. The value of P(n) for each n corresponds do the power level at that particular harmonic of the fundamental frequency.

Note also that the average power level P(n) for any frequency component n is not a function of time. Thus with conventional Fourier analysis, the concept of a frequency component, whose average amplitude varies as a function of time is not applicable.

2.1.2. FOURIER INTEGRALS Fourier integral analysis may be used to describe the frequency spectra of nonperiodic waveforms. The Fourier integral formulas are derived from the Fourier series formulas by letting the period of the waveform under analysis approach infinity. This gives infinitesimal frequency separation between the frequency components, and thus leads to a dense or continuous frequency spectrum, as opposed to the "line" spectra obtained from the Fourier series expansion.

The Fourier integral representation of a function f(t) is [1] as follows

$$f(t) = \int_0^{\infty} a(\omega) \cos \omega t \, d\omega + \int_0^{\infty} b(\omega) \sin \omega t \, d\omega \qquad (8)$$

where

$$a(\omega) = \frac{1}{\pi} \int_{-\infty}^{\infty} f(t) \cos \omega t \, dt \tag{9}$$

$$b(\omega) = \frac{1}{\pi} \int_{-\infty}^{\infty} f(t) \sin \omega t \, dt \tag{10}$$

If f(t) is a voltage which is applied across a 1-ohm resistive load, the total energy W dissipated for all time from $-\infty$ to $+\infty$ is given by

$$W = \int_{-\infty}^{\infty} [f(t)]^2 dt \tag{11}$$

In order for W to be finite, the actual duration of f(t) must also be finite. If this requirement is satisfied (as it would be for a seismic wave), the Fourier integral energy theorem [1] applies and

$$\int_{-\infty}^{\infty} [f(t)]^2 dt = \pi \int_{0}^{\infty} [a(\omega)]^2 + [b(\omega)]^2 d\omega \tag{12}$$

Substituting Equation 11 into 12 gives

$$W = \pi \int_{0}^{\infty} [a(\omega)]^2 + [b(\omega)]^2 d\omega \tag{13}$$

Equation 13 gives the total energy in f(t) as a summation of the separate energies of all the frequency components. The energy contained in all frequency components between 0 and ω_j would be given by

$$W(\omega_j) = \pi \int_{0}^{\omega_j} [a(\omega)]^2 + [b(\omega)]^2 d\omega \tag{14}$$

Since the integrand is always positive, $W(\omega_j)$ is a monotonic increasing function. This function may be plotted as shown in Figure 3.

Since the slope of the curve of Figure 3 corresponds to the increase in energy W per unit increase in angular frequency ω, the energy-density function may be obtained by differentiating Equation 14 with respect to ω_j.

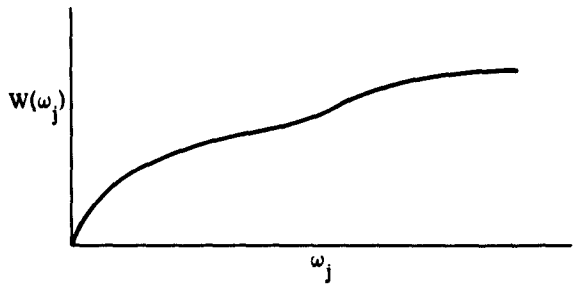

FIGURE 3. INTEGRATED ENERGY-DENSITY SPECTRUM

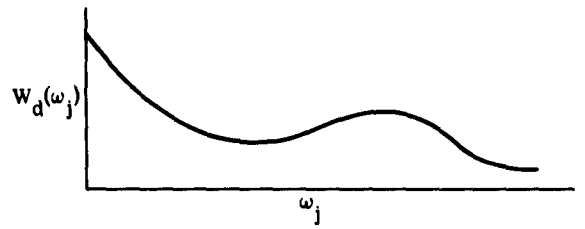

FIGURE 4. ENERGY-DENSITY SPECTRUM

$$W_d(\omega_j) = \frac{dW(\omega_j)}{d\omega_j} = \pi\left\{[a(\omega)]^2 + [b(\omega)]^2\right\} \tag{15}$$

A plot of $\frac{dW(\omega_j)}{d\omega_j}$ corresponding to the $W(\omega_j)$ function of Figure 3 is shown in Figure 4.

This plot corresponds roughly to the Fourier series power spectrum, as shown in Figure 2, except that it is a continuous spectrum instead of a line spectrum, and the ordinate is energy density instead of power.

Thus, the expression

$$W_d(\omega) = \pi\left\{[a(\omega)]^2 + [b(\omega)]^2\right\} \tag{15}$$

corresponds to energy per unit bandwidth in the frequency spectrum of f(t). The energy at any single frequency is zero, since this is given by $\pi\left\{[a(\omega)]^2 + [b(\omega)]^2\right\} d\omega$.

As in the case of Fourier series, the frequency components $a(\omega)$ and $b(\omega)$ are not functions of time. The integral

$$f(t) = \int_0^{\infty} [a(\omega) \cos \omega t + b(\omega) \sin \omega t] d\omega \qquad (8)$$

may be visualized as a summation of sinusoids of all frequencies, each sinusoid extending in time from $-\infty$ to $+\infty$. These sinusoids add to produce f(t) for the interval in time during which f(t) exists, and add to produce zero at all other times. The energy in any one of these sinusoids is zero, whereas the energy density per unit bandwidth is not, as shown by Equation 15 above. Since the sinusoids extend in time from $-\infty$ to $+\infty$, and since the energy per unit bandwidth is finite, the power per unit bandwidth is zero. If the power in any band of frequencies were greater than zero, this power integrated for time from $-\infty$ to $+\infty$ would give infinite energy!

Although Fourier integral analysis can be applied to seismic waves, and the energy-density spectrum can be plotted, the results are not particularly useful; they apply to the wave in its entirety and there is no provision for obtaining the relative intensities of the various frequency components for different portions of the seismogram as a function of time. If we wish to examine various parts of the wave trains for their frequency compositions and plot these frequency spectra as functions of time, the formal techniques of Fourier integral analysis must be modified.

2.2. TIME-VARYING POWER SPECTRA

Not all portions of a seismogram have the same frequency content. That of the initial portion of a seismogram may be completely different from that of the final portion. Thus it is desirable to be able to observe the amplitude of each frequency component as a function of time. A formal Fourier integral analysis of a seismic waveform yields a frequency spectrum which does not vary with time; therefore, a modified analytical procedure is required to obtain a time-varying spectrum.

2.2.1. NATURE OF A TIME-VARYING POWER SPECTRUM Exact specification of any general function f(t) in terms of time-varying frequency spectra is quite difficult, or even perhaps, impossible. This difficulty results from the fact that a sinusoid of constant frequency whose amplitude is varying with time cannot be regarded as a single frequency. Instead, since it is an amplitude-modulated wave, it has a frequency spectrum consisting of a carrier frequency plus bands of adjacent frequencies called sidebands [1]. If a sinusoid with a frequency ω_c is amplitude modulated by another sinusoid with a frequency ω_m, the resulting modulated signal contains three frequencies: the carrier, ω_c; the upper sideband, $\omega_c + \omega_m$; and the lower sideband, $\omega_c - \omega_m$. If the modulation envelope of the sinusoid is not itself a sinusoid, then each Fourier frequency component of the modulating signal generates an upper- and lower-sideband fre-

quency. Thus, the spectrum of the upper sideband is the same as that of the modulating signal, with all frequencies displaced upward by the amount of the carrier frequency, whereas the lower-sideband frequency spectrum is a mirror image, reflected in the carrier, of the upper sideband. These relationships are illustrated in Figure 5.

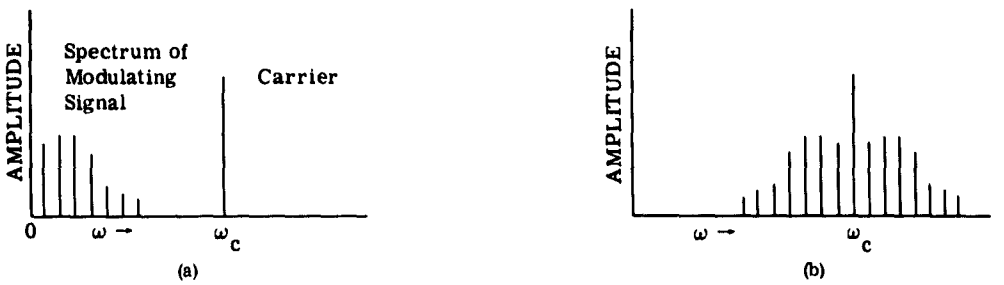

FIGURE 5. SPECTRA RESULTING FROM AMPLITUDE-MODULATION PROCESS. (a) Spectra of modulating signal and carrier. (b) Spectrum of modulated sinusoid.

The bandwidth or frequency spread occupied by the signal is determined by the highest frequency component of the modulation envelope. Consequently, if we expect to detect rapid variations in the amplitude of a given frequency component of a seismic signal, we must really examine the signal over a wide band of frequencies; therefore it becomes impossible to specify exactly what frequency component is being measured. On the other hand, if a very narrow band of frequencies is being examined, so that the frequency component whose amplitude is being measured is specified very accurately, rapid variations in the amplitude of this component cannot be detected because the sideband frequencies which are generated by the higher frequency components of the modulation envelope are being suppressed.

2.2.2. TECHNIQUES FOR COMPUTING TIME-VARYING POWER SPECTRA

2.2.2.1. The Rectangular Time Aperture. One possible method of computing the time-varying power spectrum of a signal f(t) is illustrated by Figure 6.

Suppose the actual duration of f(t) is unknown, and we wish to estimate its frequency composition at time t_o. The portion of f(t) extending from $t_o - T/2$ to $t_o + T/2$ could be analyzed to determine the energy-density spectrum for this portion of f(t). The energy-density spectrum for all of f(t) cannot be computed from this sample, but the energy contributed during this period can be computed and divided by the length of the period to give an average power-density spectrum for the interval from $t_o - T/2$ to $t_o + T/2$.

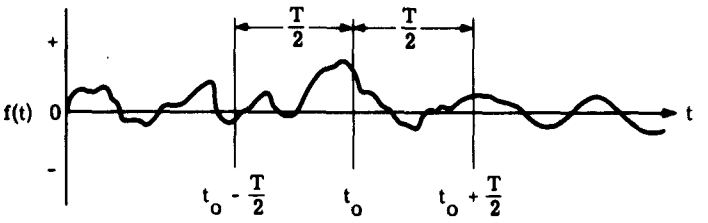

FIGURE 6. EXAMINATION OF f(t) THROUGH A "TIME WINDOW"

Thus, if we consider f(t) as existing only in the interval $(t_o - T/2) < t < (t_o + T/2)$, we can compute the energy-density spectrum as follows: changing the limits for the integrals of Equations 8 and 9, and considering the results as a function of t_o we derive

$$a(\omega, t_o) = \frac{1}{\pi} \int_{t_o - T/2}^{t_o + T/2} f(t) \cos \omega t \, dt \tag{16}$$

$$b(\omega, t_o) = \frac{1}{\pi} \int_{t_o - T/2}^{t_o + T/2} f(t) \sin \omega t \, dt \tag{17}$$

The energy-density spectrum is given by Equation 15:

$$W_d(\omega) = \pi \left\{ [a(\omega)]^2 + [b(\omega)]^2 \right\} \tag{15}$$

and the average power-density spectrum at t_o may be obtained by dividing by the length of the interval:

$$P(\omega, t_o) = \frac{\pi}{T} \left\{ [a(\omega, t_o)]^2 + [b(\omega, t_o)]^2 \right\} \tag{18}$$

Substituting Equations 16 and 17 into Equation 18 gives

$$P(\omega, t_o) = \frac{1}{\pi T} \left\{ \left[\int_{t_o - T/2}^{t_o + T/2} f(t) \cos \omega t \, dt \right]^2 + \left[\int_{t_o - T/2}^{t_o + T/2} f(t) \sin \omega t \, dt \right]^2 \right\} \tag{19}$$

The integrals in Equation 19 could be evaluated continuously on analog computing equipment for any specified ω as a function of t_o by using tape-recording equipment with spaced playback heads, so that the

integrals of f(t) could be obtained simultaneously between the limits of 0 and $t_o + \frac{T}{2}$, and of 0 and $t_o - \frac{T}{2}$. The first integral of Equation 19 can be rewritten

$$\int_{t_o-T/2}^{t_o+T/2} f(t) \cos \omega t \, dt = \int_0^{t_o+T/2} f(t) \cos \omega t \, dt - \int_0^{t_o-T/2} f(t) \cos \omega t \, dt \tag{20}$$

providing f(t) is continuous from 0 to $t_o + T/2$, and $t_o - T/2 > 0$.

Substituting $t + T/2$ for t in the first integral on the right side of Equation 20 gives

$$\int_0^{t_o+T/2} f(t) \cos \omega t \, dt = \int_{-T/2}^{t_o} f(t + T/2) \cos \omega(t + T/2) \, dt \tag{21}$$

Similarly, the second integral may be written

$$\int_0^{t_o-T/2} f(t) \cos \omega t \, dt = \int_{T/2}^{t_o} f(t - T/2) \cos \omega(t - T/2) \, dt \tag{22}$$

If $f(t) = 0$ for $t < 0$, then $f(t - T/2) = 0$ for $t < T/2$, and the lower limit of the integral on the right in Equation 22 may be extended to $-T/2$ without affecting the value of the result. Therefore, substituting Equations 21 and 22 in 20 gives

$$\int_{t_o-T/2}^{t_o+T/2} f(t) \cos \omega t \, dt = \int_{-T/2}^{t_o} [f(t + T/2) \cos \omega(t + T/2) - f(t - T/2) \cos \omega(t - T/2)] \, dt \tag{23}$$

Equation 23 could easily be mechanized on analog computing equipment in combination with a tape recorder having two playback heads spaced T seconds apart, so that $f(t + T/2)$ and $f(t - T/2)$ could be obtained.

A similar method could be used to obtain

$$\int_{t_o-T/2}^{t_o+T/2} f(t) \sin \omega t \, dt \tag{24}$$

and $P(\omega, t_o)$ as a continuous function of t_o could be computed from Equation 19.

There would be no need for a tape recorder if a device having a transport delay of T seconds were available. A block diagram showing the method of computing the first integral of Equation 19 be using such a device is shown in Figure 7.

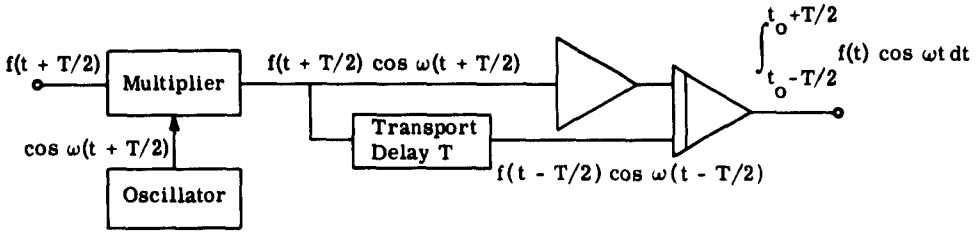

FIGURE 7. ANALOG-COMPUTER MECHANIZATION OF EQUATION 23

2.2.2.2. The Rectangular Frequency Aperture. The power spectrum of f(t) as a function of time might also be found by use of a filter. For example, a filter having a finite passband with sharp cutoff at the edges of the passband might be regarded as a rectangular aperture or "window" for viewing the frequency spectrum of f(t). Figure 8 shows the passband of such a filter superimposed upon $P(\omega)$, the power spectrum of f(t).

The filter, whose pass charcteristic is shown in Figure 8, passes all frequencies from $\omega_o - \frac{\Delta\omega}{2}$ to $\omega_o + \frac{\Delta\omega}{2}$ without attenuation, and completely suppresses all frequencies outside this range. If the filter function is $G(\omega - \omega_o)$, the power transmitted through the filter is given by

$$p(\Delta\omega) = \int_0^\infty p(\omega) G(\omega - \omega_o)\, d\omega = \int_{\omega_o - \frac{\Delta\omega}{2}}^{\omega_o + \frac{\Delta\omega}{2}} p(\omega)\, d\omega \qquad (25)$$

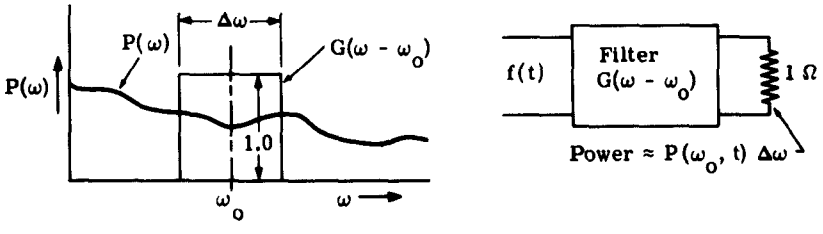

FIGURE 8. ILLUSTRATION OF A FREQUENCY APERTURE

and the average power per unit bandwidth for the frequency range covered by the filter is obtained by dividing Equation 25 by $\Delta\omega$.

$$P(\omega_o, t) = \frac{1}{\Delta\omega} \int_{\omega_o - \frac{\Delta\omega}{2}}^{\omega_o + \frac{\Delta\omega}{2}} P(\omega)\, d\omega \tag{26}$$

The output of the filter may be time-varying, subject to restrictions imposed by the filter's bandpass characteristics. The filter should have a narrow passband in order to restrict the range of ω over which the power is averaged for any given ω_o, and thus give good frequency resolution. However, if the passband is very narrow, rapid variations of the power output cannot be transmitted because the sideband frequencies which must be part of such a signal are suppressed.

In practice, the filter would be set for various values of ω_o, and the output power would be interpreted as $\Delta\omega\ P(\omega_o, t)$.

2.2.2.3. Comparison of Time-Aperture and Frequency-Aperture Approaches. Summarizing Sections 2.2.1 and 2.2.2, it appears that there are two possible methods of obtaining time-varying power-density spectra of f(t). One of these involves examination of a portion of f(t) through a moving "window" in time and performing Fourier integral analysis on the portion of f(t) seen through the window. The second involves use of a filter, or frequency-spectrum window, through which the power content of a band of frequency components of f(t) are observed. The entire frequency spectrum could be covered either by using a number of filters, or by adjusting the center frequency of a single filter and making consecutive observations.

Increasing the length of the time window for the first method improves the accuracy of frequency-component determination, but reduces the rate at which the power density being measured can vary. Increasing the length of the frequency window for the second method has the opposite effect. It increases the rate at which the output of the filter may vary but reduces the selectivity, or frequency resolution.

It will be shown later that the two methods discussed above are not really separate and that any method of analyzing a signal f(t) in terms of a time-varying frequency spectrum involves the use of both a time aperture and a frequency aperture.

2.2.2.4. The Variable-Transmission Time Aperture. Use of the rectangular time aperture, as described in Section 2.2.1, gives the average power-density spectrum of f(t) for the interval $(t_o - T/2) \leq t \leq (t_o + T/2)$. In determining this average $P(\omega, t_o)$, equal weight is given to the spectral characteristics of f(t) throughout the interval covered by the time aperture. Better time resolution would result if the spec-

tral characteristics of f(t) in the neighborhood of t_o were emphasized in the computing process. This may be accomplished by using a variable-transmission time aperture whose transmission is maximum in the neighborhood of t_o. An equation for computing $P(\omega, t_o)$, which uses a time aperture of this type, will be derived in this section.

In deriving this formula, it is comvenient to use the exponential form of the Fourier series and integral formulas. For the Fourier series, these are [2]

$$f(t) = \sum_{n=-\infty}^{\infty} F(n)e^{jn\omega_1 t} \tag{27}$$

$$F(n) = \frac{1}{T}\int_{-T/2}^{T/2} f(t)e^{-jn\omega_1 t}\,dt \tag{28}$$

$$F(n) = \frac{1}{2}(A_n - jB_n) \qquad (n = 0, \pm 1, \pm 2, \ldots) \tag{29}$$

where A_n and B_n correspond to the coefficients of the trigonometric series (Equation 1). The factor of 1/2 occurs in Equation 29 because the exponential form of the series uses both negative and positive values of n, and thus has twice as many terms as the trigonometric series, which uses only positive values of n.

If f(t) is the voltage across, or the current through a 1-ohm resistor, the average power dissipated in the resistor by the n-th harmonic component is

$$p(n) = |F(n)|^2 = \frac{A_n^2 + B_n^2}{4} \qquad (n = 0, \pm 1, \pm 2, \ldots) \tag{30}$$

Comparison of Equation 30 with Equation 6 reveals that the p(n) of the former is equal to half the p(n) of the latter. Similarly, any time-varying continuous power spectrum derived from the exponential formulas will include both positive and negative values of ω, and therefore the value of $p(\omega_o, t_o)$ so obtained must be doubled to obtain $P(\omega_o, t_o)$, the physical power level at frequency ω_o at time t_o.

Substituting Equation 28 into Equation 30 gives

$$p(n) = |F(n)|^2 = \frac{1}{T^2}\left|\int_{-T/2}^{T/2} f(t)e^{-jn\omega_1 t}\,dt\right|^2 \tag{31}$$

where

$$\omega_1 = 2\pi f_1 = \frac{2\pi}{T}$$

and is the fundamental frequency.

Equation 31 gives the power level of each frequency component. Since each harmonic frequency is an integral multiple of the fundamental frequency, a plot of p(n) versus n would be a "line" spectrum, with ω_1 as the spacing between adjacent lines.

Even if f(t), is nonperiodic, the Fourier components for a section of f(t) extending from -T/2 to T/2 are still given by Equation 31. The length of the section under consideration may be extended by increasing T. When T is increased, ω_1 is decreased, thus reducing the spacing of lines on the power spectrum. As T is allowed to approach infinity, ω_1 approaches zero and the power spectrum becomes a continuous plot. Since there are now an infinite number of frequency components in any finite bandwidth, and the power in such a bandwidth is also finite, the power per frequency component must be zero.

Thus,

$$\lim_{T\to\infty} p(n) = \lim_{T\to\infty} \frac{1}{T^2} \left| \int_0^T f(t) e^{-jn\omega_1 t}\, dt \right|^2 = 0 \qquad (32)$$

Thus, the power spectrum can no longer be expressed in terms of power per frequency component. In order to avoid this difficulty, the power density at any given frequency may be expressed in terms of power per unit bandwidth.

If p(n) = power per frequency component, and the frequency components are spaced f_1 cps apart, the number of frequency components per cps is $1/f_1$, and the number of frequency components per radian per second is $1/\omega_1 = 1/2\pi f_1$. The power density in watts per radian per second, then, is $p(n\omega_1) = \frac{p(n)}{2\pi f_1}$.

Substituting this into Equation 31 gives

$$p(n\omega_1) = \frac{1}{2\pi f_1 T^2} \left| \int_{-T/2}^{T/2} f(t) e^{-jn\omega_1 t}\, dt \right|^2 \qquad (33)$$

or, since $f_1 = 1/T$,

$$p(n\omega_1) = \frac{1}{2\pi T} \left| \int_{-T/2}^{T/2} f(t) e^{-jn\omega_1 t}\, dt \right|^2$$

Then, in order to obtain a continuous frequency spectrum, let T become infinite. The quantity $n\omega_1$, becomes ω, and

$$p(\omega) = \lim_{T\to\infty} \frac{1}{2\pi T} \left| \int_{-T/2}^{T/2} f(t) e^{-j\omega t} dt \right|^2 \tag{34}$$

At this point, a brief discussion of the nature of the function defined by Equation 34 is in order. It may be shown that this function is not valid as a statistical estimate of the power spectrum of a random process, because the variance of the $p(\omega)$ defined in this manner does not approach zero as T becomes infinite, [3]. Nevertheless, Equation 34 accurately defines the power spectrum of the particular function, f(t), to which the equation is applied in that the power spectrum so defined corresponds exactly to the spectral density of the Fourier series for f(t). The function, $p(\omega)$, as defined by Equation 34 is extremely irregular. Since $p(\omega)$ is proportional to the amplitudes of the Fourier series components making up f(t), and since f(t) is infinitely long, the increment between terms of the series is infinitesimal, and thus any small interval of ω (no matter how small) contains an infinite number of different values for $p(\omega)$. If $p(\omega)$ is averaged over a small increment of ω, however, a consistent usable value for average $p(\omega)$ for that interval is obtained. According to Goldman, [4], this averaged or smoothed power spectrum

$$\overline{p(\omega)} = \lim_{\Delta\omega\to 0} \frac{1}{\Delta\omega} \int_{\omega}^{\omega+\Delta\omega} p(\omega)\, d\omega$$

corresponds to the statistical power spectrum for the function f(t). In other words, $\overline{p(\omega)}$ as defined above is also the result of averaging $p(\omega)$ from Equation 34 for an infinite number of random functions of time, each having the same statistical power spectrum. In the steps which follow, since the sections of f(t) being examined are of finite length, an averaging with respect to ω always occurs, and we are not bothered by a variance of $p(\omega)$ of the type discussed above.

Next, let us consider the problem of estimating $p(\omega)$ by observing a finite section of f(t). If f(t) has uniform power spectral characteristics throughout the length T of the section being observed,

$$p(\omega) \approx \frac{1}{2\pi T} \left| \int_{-T/2}^{T/2} f(t) e^{-j\omega t} dt \right|^2 \tag{35}$$

for $\omega >> \frac{2\pi}{T}$.

Since T is now finite, we are really formally justified in computing the frequency spectrum only at values of ω which are multiples of the fundamental frequency $\omega_1 = 2\pi/T$. Evidently, the resolution of the frequency spectrum obtained from Equation 35 is of the order of 1/T cps. Roughly, about 1% resolution could be obtained if T corresponded to 100 cycles of ω, the frequency for which the power density is to be

computed. If $p(\omega)$ is to be determined accurately at low frequencies, long intervals of $f(t)$ must be observed; but for higher frequencies, the interval T can be shortened.

If a portion of the time axis of $f(t)$ is divided into a number of intervals, each long enough to permit a reasonably accurate computation of $p(\omega)$ using Equation 35, and if the power density spectrum of $f(t)$ is uniform throughout the portion chosen, then the values of $p(\omega)$ obtained by applying Equation 35 to each of the intervals should be approximately the same.

For each interval, extending from time t_{n-1} to t_n, Equation 35 may be written

$$p(\omega) \approx \frac{1}{2\pi(t_n - t_{n-1})} \left| \int_{t_{n-1}}^{t_n} f(t)e^{-j\omega t}dt \right|^2 \tag{36}$$

or

$$2\pi(t_n - t_{n-1})\, p(\omega) \approx \left| \int_{t_{n-1}}^{t_n} f(t)e^{-j\omega t}dt \right|^2 \tag{37}$$

Summing all equations of this type from n = 1 to n = N, where $t_N - t_o = T$, and assuming that $p(\omega)$ is constant over this interval, we derive

$$2\pi(\omega) \sum_{n=1}^{N} (t_n - t_{n-1}) \approx \sum_{n=1}^{N} \left| \int_{t_{n-1}}^{t_n} f(t)e^{-j\omega t}dt \right|^2 \tag{38}$$

However,

$$\sum_{n=1}^{N} (t_n - t_{n-1}) = T \tag{39}$$

therefore,

$$2\pi p(\omega)\, T \approx \sum_{n=1}^{N} \left| \int_{t_{n-1}}^{t_n} f(t)e^{-j\omega t}dt \right|^2 \tag{40}$$

And substituting Equation 40 into Equation 35 gives

$$\left| \int_{-T/2}^{T/2} f(t)e^{-j\omega t}dt \right|^2 \approx \sum_{n=1}^{N} \left| \int_{t_{n-1}}^{t_n} f(t)e^{-j\omega t}dt \right|^2 \tag{41}$$

An integral over any interval may be expressed as the sum of integrals over all subintervals contained in this interval; thus

$$\int_{-T/2}^{T/2} f(t)e^{-j\omega t}dt = \sum_{n=1}^{N} \int_{t_{n-1}}^{t_n} f(t)e^{-j\omega t}dt \tag{42}$$

The operation of squaring the absolute values of both sides of Equation 42 and substituting the result into Equation 41 gives the rather interesting relation

$$\left|\sum_{n=1}^{N} \int_{t_{n-1}}^{t_n} f(t)e^{-j\omega t}dt\right|^2 = \sum_{n=1}^{N} \left|\int_{t_{n-1}}^{t_n} f(t)e^{-j\omega t}dt\right|^2 \tag{43}$$

If $(t_n - t_{n-1}) = \Delta t$ (with all intervals equal), and thus

$$\sum_{n=1}^{N} (t_n - t_{n-1}) = T = N\Delta t$$

then Equation 38 can be rewritten to give

$$p(\omega) = \frac{\sum_{n=1}^{N} \frac{1}{2\pi\Delta t} \left|\int_{t_{n-1}}^{t_n} f(t)e^{-j\omega t}dt\right|^2}{N} \tag{44}$$

Thus, this gives $p(\omega)$ for the interval from $t = 0$ to $t = N\Delta t$ as the average of the values of $p(\omega)$ computed for the subintervals $t_{n-1} < t < t_n$.

If the power spectrum of f(t) varies with time, Equation 44 specifies the average value of $p(\omega)$ for the section of f(t) being examined. In order to define $p(\omega)$ at some particular time t_o, a weighting function may be used in computing this average. Suppose we use a weighting function $Q(t - t_o)$, which reaches a maximum for some particular instant t_o and approaches zero for values of t which are significantly removed from t_o, in such a manner that the integral $\int_{-\infty}^{\infty} Q(t - t_o)dt$ exists. (Figure 9 shows a typical weighting function.) Use of such a weighting function will give more weight to the spectral characteristics of f(t) in the neighborhood of $t = t_o$, and thus the weighted average of $p(\omega)$, obtained by using this weighting function, can be interpreted as $p(\omega)$ at $t = t_o$.

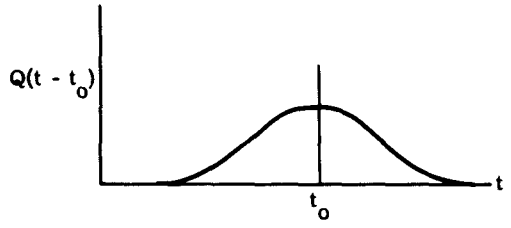

FIGURE 9. A WEIGHTING FUNCTION

Using the weighting function $Q(t - t_o)$, Equation 44 can be rewritten

$$p(\omega, t_o) = \frac{\sum_{n=1}^{N} Q(t_n - t_o) \frac{1}{2\pi\Delta t} \left| \int_{t_{n-1}}^{t_n} f(t)e^{-j\omega t} dt \right|^2}{\sum_{n=1}^{N} Q(t_n - t_o)} \tag{45}$$

where $Q(t_n - t_o)$ is the average value of the weighting function in the interval $t_{n-1} < t < t_n$.

Since $Q(t_n - t_o)$ is constant for any particular t_n, Equation 45 can be rewritten

$$p(\omega, t_o) = \frac{\sum_{n=1}^{N} \frac{1}{2\pi} \left| \int_{t_{n-1}}^{t_n} \sqrt{Q(t_n - t_o)}\, f(t)e^{-j\omega t} dt \right|^2}{\sum_{n=1}^{N} Q(t_n - t_o)\Delta t} \tag{46}$$

If N is permitted to increase now, so that Equation 46 includes all time from $-\infty$ to ∞, Equation 46 can be rewritten

$$p(\omega, t_o) = \frac{\sum_{n=-\infty}^{\infty} \frac{1}{2\pi} \left| \int_{t_{n-1}}^{t_n} \sqrt{Q(t_n - t_o)}\, f(t)e^{-j\omega t} dt \right|^2}{\sum_{n=-\infty}^{\infty} Q(t_n - t_o)\Delta t} \tag{47}$$

and, when Equation 41 is used,

$$p(\omega, t_o) = \frac{\frac{1}{2\pi}\left|\int_{-\infty}^{\infty} \sqrt{Q(t - t_o)}\, f(t) e^{-j\omega t} dt\right|^2}{\sum_{n=-\infty}^{\infty} Q(t_n - t_o)\Delta t} \tag{48}$$

Finally, if we allow Δt in the denominator of Equation 48 to approach zero,

$$p(\omega, t_o) = \frac{\frac{1}{2\pi}\left|\int_{-\infty}^{\infty} \sqrt{Q(t - t_o)}\, f(t) e^{-j\omega t} dt\right|^2}{\int_{-\infty}^{\infty} Q(t - t_o)\, dt} \tag{49}$$

and, if we redefine $\sqrt{Q(t - t_o)} = f_1(t - t_o)$,

$$p(\omega, t_o) = \frac{\frac{1}{2\pi}\left|\int_{-\infty}^{\infty} f_1(t - t_o) f(t) e^{-j\omega t} dt\right|^2}{\int_{-\infty}^{\infty} f_1^{\,2}(t - t_o)\, dt} \tag{50}$$

For any specified weighting function, the denominator of the right side of Equation 50 is a constant:

$$\int_{-\infty}^{\infty} f_1^{\,2}(t - t_o)\, dt = \frac{1}{K} \tag{51}$$

So, this equation can be rewritten

$$p(\omega, t_o) = \frac{K}{2\pi}\left|\int_{-\infty}^{\infty} f_1(t - t_o) f(t) e^{-j\omega t} dt\right|^2 \tag{52}$$

where

$$K = \frac{1}{\int_{-\infty}^{\infty} f_1^{\,2}(t - t_o)\, dt} \tag{53}$$

Equation 52 can be interpreted as describing the use of an aperture or window in time, having a transmission function of $f_1(t - t_o)$ to examine f(t) about the instant t_o and to determine the power spectrum of f(t) at that point.

If $f_1(t - t_o) = 1$ for all values of t and t_o, Equation 52 becomes equivalent to Equation 34, which is restated here:

$$p(\omega) = \lim_{T\to\infty} \frac{1}{2\pi T} \left| \int_{-T/2}^{T/2} f(t) e^{-j\omega t} dt \right|^2 \tag{34}$$

Thus we obtain the non-time-varying power-density spectrum, where $p(\omega)$ is the average power density at ω for all time, from $-\infty$ to $+\infty$.

Evidently, the time resolution of $p(\omega, t_o)$ as computed from Equation 52 is improved as the interval covered by the window function $f_1(t - t_o)$ becomes narrower, but a resonably long window function must be used to give good frequency resolution.

2.2.2.5. The Frequency-Aperture Equivalent of a Time Aperture. Next, we show that use of a time aperture in the manner specified by Equation 52 is actually equivalent to using a window in the frequency domain.

For power at a specific time t_o and at a specific frequency ω_o, Equation 52 is written

$$p(\omega_o, t_o) = \frac{K}{2\pi} \left| \int_{-\infty}^{\infty} f_1(t - t_o)\, f(t) e^{-j\omega_o t} dt \right|^2 \tag{54}$$

Substituting $\tau + t_o$ for t in the integrand of Equation 54 gives

$$p(\omega_o, t_o) = \frac{K}{2\pi} \left| e^{-j\omega_o t_o} \int_{-\infty}^{\infty} f(\tau + t_o)\, f_1(\tau) e^{-j\omega_o \tau} d\tau \right|^2 \tag{55}$$

Since ω_o is a constant for this integration, we can define

$$f_2(\tau) = f_1(\tau) e^{-j\omega_o \tau} \tag{56}$$

Substituting this in Equation 55 gives

$$p(\omega_o, t_o) = \frac{K}{2\pi} \left| e^{-j\omega_o t_o} \int_{-\infty}^{\infty} f(\tau + t_o)\, f_2(\tau)\, d\tau \right|^2 \tag{57}$$

However, it can be shown [2] that

$$\int_{-\infty}^{\infty} f_2(\tau) f(\tau + t_o)\, d\tau = \int_{-\infty}^{\infty} 2\pi\, \bar{F}_2(\omega) F(\omega) e^{j\omega t_o} d\omega \tag{58}$$

where

$$F(\omega) = \frac{1}{2\pi} \int_{-\infty}^{\infty} f(\tau) e^{-j\omega\tau} d\tau \tag{59}$$

$$F_2(\omega) = \frac{1}{2\pi}\int_{-\infty}^{\infty} f_2(\tau)e^{-j\omega\tau}\,d\tau \tag{60}$$

$$\bar{F}_2(\omega) = \frac{1}{2\pi}\int_{-\infty}^{\infty} \bar{f}_2(\tau)e^{j\omega\tau}\,d\tau \tag{61}$$

Since by definition,

$$\bar{f}_2(\tau) = f_1(\tau)e^{j\omega_o\tau} \tag{56}$$

Equation 61 can be rewritten

$$\bar{F}_2(\omega) = \frac{1}{2\pi}\int_{-\infty}^{\infty} f_1(\tau)e^{j(\omega+\omega_o)\tau}\,d\tau$$

$$= \bar{F}_1(\omega + \omega_o) \tag{62}$$

Substituting Equation 62 into Equation 58 and the result into Equation 57,

$$p(\omega_o, t_o) = \frac{K}{2\pi}\left|e^{-j\omega_o t_o}\int_{-\infty}^{\infty} 2\pi F(\omega)\bar{F}_1(\omega + \omega_o)e^{j\omega t}\,d\omega\right|^2 \tag{63}$$

and, since $\left|e^{-j\omega_o t_o}\right| = 1$

$$p(\omega_o, t_o) = 2\pi K\left|\int_{-\infty}^{\infty} F(\omega)\bar{F}_1(\omega + \omega_o)e^{j\omega t}\,d\omega\right|^2 \tag{64}$$

The factor K in Equation 64 can be rewritten in terms of $\bar{F}_1(\omega + \omega_o)$ by using the Fourier integral energy theorem.

Since $f_1(\tau)$ and $F_1(\omega + \omega_o)$ are a Fourier transform pair,

$$\frac{1}{K} = \int_{-\infty}^{\infty} f_1^2(t - t_o)\,dt = \int_{-\infty}^{\infty} f_1^2(\tau)\,d\tau = \int_{-\infty}^{\infty} 2\pi\left|F_1(\omega + \omega_o)\right|^2 d\omega \tag{65}$$

and since

$$\left|F_1(\omega + \omega_o)\right| = \left|\bar{F}_1(\omega + \omega_o)\right| \tag{66}$$

therefore

$$K = \frac{1}{2\pi \int \left| F_1(\omega + \omega_o) \right|^2 d\omega} \tag{67}$$

Substituting Equation 67 into Equation 64, substituting $-\omega_o$ for ω_o in the result, and recalling that $p(\omega_o, t_o) = p(-\omega_o, t_o)$ because of symmetry in the power spectrum, we obtain:

$$p(\omega_o, t_o) = p(-\omega_o, t_o) = \frac{\left| \int_{-\infty}^{\infty} \bar{F}_1(\omega - \omega_o) F(\omega) e^{j\omega t_o} d\omega \right|^2}{\int_{-\infty}^{\infty} \left| F_1(\omega - \omega_o) \right|^2 d\omega} \tag{68}$$

Repeating Equation 50 for comparison,

$$p(\omega_o, t_o) = \frac{\frac{1}{2\pi} \left| \int_{-\infty}^{\infty} f_1(t - t_o) f(t) e^{-j\omega_o t} dt \right|^2}{\int_{-\infty}^{\infty} f_1^2(t - t_o) dt} \tag{50}$$

In comparing Equations 50 and 68, we see clearly that since Equation 50 describes $p(\omega_o, t_o)$ in terms of a portion of f(t) as seen through a variable-transmission "time-window" function $f_1(t - t_o)$, Equation 68 describes $P(\omega_o, t_o)$ in terms of a portion of $F(\omega)$, the spectrum of F(t) as seen through a variable-transmission "frequency-window" function $\bar{F}_1(\omega - \omega_o)$. The frequency window $\bar{F}_1(\omega - \omega_o)$ is the complex conjugate of the Fourier transform of the time window, $f_1(t - t_o)$.

In general, if the time aperture is narrowed in order to obtain better time resolution, the effective filter bandwidth is broadened, and the frequency resolution becomes poorer. If the time aperture is widened so that the frequency spectrum is computed for larger sections of f(t), the frequency resolution is improved, but the time response or resolution is degraded. Specification of either the time aperture or the filter bandwidth characteristic determines both, since one is derived from the other. The exact choice of either aperture depends upon the nature of the data to be analyzed and the type of spectral information desired.

2.2.3. THE FREQUENCY-ANALYSIS METHOD USED IN THE IST ANALOG COMPUTER LABORATORY

2.2.3.1. Computer Setup. In preparation for measurement of its power spectrum on the analog computer, the seismic signal to be analyzed was first recorded on one channel of a length of magnetic tape. The ends of this length of tape were spliced together to form a loop so that when the loop was played back, the recorded seismic signal would be reproduced repeatedly. Control signals were recorded on a second channel of the tape at positions corresponding to the beginning and ending of the seismic signal. These control signals were used to program the operation of the analog computer.

The computer was so mechanized that it examined a different segment of the power spectrum of the seismic signal for each pass of the tape, and plotted the results automatically. The control signals which were recorded on the second channel of the tape actuated the analog computer so that it automatically reset itself to a new "interrogation" frequency for each pass of the tape. Thus, each pass of the tape generated information concerning a new portion of the power spectrum.

Figure 10 is a block diagram of the basic computing circuit used. The oscillator, operating at some interrogation frequency ω_i, generates signals corresponding to cos $\omega_i t$ and sin $\omega_i t$. Multiplier A multiplies the incoming seismic signal f(t) by cos $\omega_i t$, whereas multiplier B multiplies f(t) by sin $\omega_i t$.

The output signal of multiplier A (designated E_1 on the diagram) next passes through filter A, and the filtered signal E_3 is squared in multiplier C to produce E_5, which is fed into the adder.

The output of multiplier B is similarly processed to produce a second input to the adder.

2.2.3.2. Theory of Computer Circuit Operation. The operation of the circuit can be explained qualitatively in terms of heterodyning and filtering. Multiplication of f(t) by cos $\omega_i t$ shifts its frequency spectrum, $F(\omega)$, by ω_i so that the frequency spectrum of E_1 is $F(\omega - \omega_i)$. Therefore, examination of the frequency spectrum of E_1 for zero frequency or d-c components is equivalent to examination of f(t) for ω_i components.

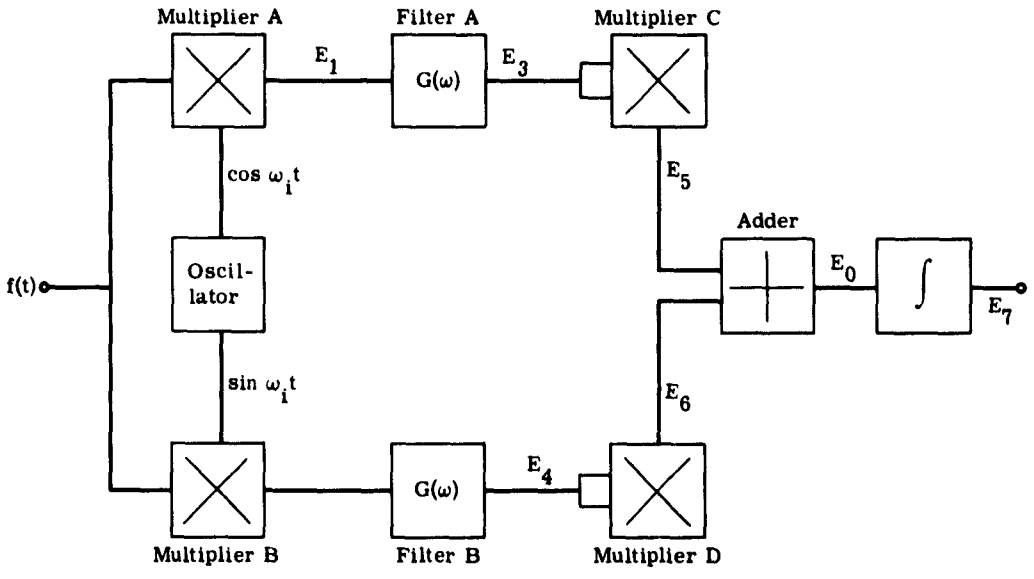

FIGURE 10. FUNCTIONAL BLOCK DIAGRAM OF ANALOG-COMPUTER CIRCUIT USED IN FREQUENCY ANALYSIS

Filter A is a low-pass filter which passes d-c perfectly but attenuates a-c signals. Use of this multiplier and lowpass filter is roughly equivalent to using a passband filter centered at ω_i on f(t) directly. The output of filter A is squared by multiplier C, thus converting voltage amplitude to power.

The lower channel operates similarly, except that it multiplies f(t) by sin $\omega_i t$ and produces a signal (E_2) having a frequency spectrum which is in phase quadrature with that of (E_1). After this signal is passed through lowpass filter B and squared, it is added to the squared signal from the upper channel and the sum is then a voltage which is proportional to $p(\omega_i, t)$.

A more quantitative explanation of the operation of the analog-computer circuit can be made by showing that it evaluates $p(\omega_i, t_o)$ in terms of Equation 52, which was derived above. Rewriting Equation 52,

$$p(\omega_i, t_o) = \frac{K}{2\pi} \left| \int_{-\infty}^{\infty} f_1(t - t_o) f(t) e^{-j\omega_i t} dt \right| \tag{52}$$

where

$$K = \frac{1}{\int_{-\infty}^{\infty} f_1^2(t - t_o)\, dt} \tag{53}$$

and where $f_1(t - t_o)$ is the time-aperture function

f(t) is the function being analyzed

ω_i and t_o are the frequency and time coordinates at which p is being evaluated

Since $e^{-j\omega_i t} = \cos \omega_i t - j \sin \omega_i t$, Equation 52 can be rewritten

$$p(\omega_i, t_o) = \frac{K}{2\pi} \left| \int_{-\infty}^{\infty} f_1(t - t_o) f(t) \cos \omega_i t\, dt - j \int_{-\infty}^{\infty} f_1(t - t_o) f(t) \sin \omega_i t\, dt \right|^2 \tag{69}$$

And, since the square of the magnitude of a complex quantity is equal to the sum of the squares of its real and imaginary components,

$$p(\omega_i, t_o) = \frac{K}{2\pi} \left\{ \left| \int_{-\infty}^{\infty} f_1(t - t_o) f(t) \cos \omega_i t\, dt \right|^2 + \left| \int_{-\infty}^{\infty} f_1(t - t_o) f(t) \sin \omega_i t\, dt \right|^2 \right\} \tag{70}$$

Returning now to Figure 10, if filter A is linear (so that superposition principles are applicable), the output signal E_3 at time t_o can be expressed in terms of the input signal $E_1(t)$ and the response of filter A to a unit impulse h(t) [2, pp. 323-328].

$$E_3(t) = \int_{-\infty}^{\infty} E_1(t)h(t_o - t)\,dt \tag{71}$$

but

$$E_1(t) = f(t) \cos \omega_i t$$

Therefore,

$$E_3(t) = \int_{-\infty}^{\infty} h(t_o - t)f(t) \cos \omega_i t\,dt \tag{72}$$

or

$$E_3(t) = \int_{-\infty}^{\infty} h[-(t - t_o)]\, f(t) \cos \omega_i t\,dt \tag{73}$$

If now we define

$$h[-(t - t_o)] = f_1(t - t_o) \tag{74}$$

and make the substitution in Equation 73, the result is

$$E_3(\omega_i, t_o) = \int_{-\infty}^{\infty} f_1(t - t_o)f(t) \cos \omega_i t\,dt \tag{75}$$

By a similar process, if the impulse response of filter B is the same as that of filter A,

$$E_4(\omega_i, T_o) = \int_{-\infty}^{\infty} f_1(t - t_o)f(t) \sin \omega_i t\,dt \tag{76}$$

Substituting Equations 75 and 76 into Equation 70 gives

$$p(\omega_i, t_o) = \frac{K}{2\pi}\left(E_3^{\,2} + E_4^{\,2}\right) \tag{77}$$

Since Figure 10 shows that

$$E_0 = E_3^{\,2} + E_4^{\,2} \tag{78}$$

then

$$p(\omega_1, t_o) = \frac{K}{2\pi} E_0(\omega_1, t_o) \tag{79}$$

where $p(\omega_1, t_o)$ is the magnitude of the time-varying power spectrum as defined by Equation 70 for time t_o and angular frequency ω_1.

and

$$K = \frac{1}{\int_{-\infty}^{\infty} f_1^2(t - t_o)\,dt}$$

In this last expression

$$f_1(t - t_o) = h[-(t - t_o)]$$

where $h(t - t_o)$ is the response of the filters to a unit impulse occurring at time t_o.

Thus, the analog-computer circuit evaluates $P(\omega_1, t_o)$ in accordance with Equation 70, and uses a time aperture or weighting function which is equivalent to the filter's input response, folded about the ordinate $t = t_o$. The relationship between $h(t - t_o)$ and $f_1(t - t_o)$ is shown in Figure 11.

2.2.3.3. Computer Circuit Operation Using First-Order Lowpass Filters. In Equation 79 above, it is assumed that the filter impulse response is such that the time-window function, $f_1(t - t_o) = h[-(t - t_o)]$, gives more weight to the characteristics of f(t) in the neighborhood of t_o and less weight to the parts of f(t) which precede t_o. Next, we shall examine the effects of using various filter transfer functions.

A first-order low-pass filter is easily synthesized from an analog integrator and two coefficient potentiometers, as shown in Figure 12.

If the integrator output is e_o, its input is $-\frac{de}{dt}$, and thus the circuit solves the equation

$$-\frac{de_o}{dt} = \alpha e_i + \alpha e_o \tag{80}$$

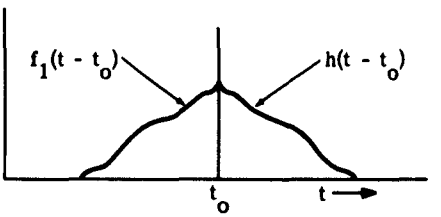

FIGURE 11. RELATIONSHIP BETWEEN $h(t - t_0)$ AND $f_1(t - t_0)$

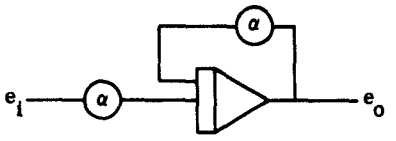

FIGURE 12. ANALOG-COMPUTER MECHANIZATION OF A LOW-PASS FILTER

If we take the Laplace transform of both sides of Equation 80 and assume that $e_o(o) = o$,

$$-s\, e_o(s) = \alpha e_i(s) + \alpha e_o(s) \tag{81}$$

and, solving for $\frac{e_o(s)}{e_i(s)}$

$$\frac{e_o(s)}{e_i(s)} = -\frac{\alpha}{\alpha + s} = -\frac{1}{1 + \frac{s}{\alpha}} \tag{82}$$

If $s = j\omega$,

$$\frac{e_o}{e_i}(j\omega) = -\frac{1}{1 + \frac{j\omega}{\alpha}} \tag{83}$$

The half-power points, where $\left|\frac{e_o}{e_i}(j\omega)\right| = \frac{1}{\sqrt{2}}$, occur at $\omega = \pm\alpha$. Therefore, the effective bandwidth of such a filter when it is used in the circuit of Figure 10 will be 2α.

The impulse response is found by taking the inverse Laplace transform of the transfer function:

$$h(t) = \mathcal{L}^{-1}\frac{\alpha}{\alpha + s} = \alpha e^{-\alpha t} \qquad (t > 0) \tag{84}$$

Then, the equivalent time-aperture function is given by

$$f_1(t - t_o) = h[-(t - t_o)] \tag{85}$$

Since

$$\begin{aligned} h(t - t_o) &= \alpha e^{-\alpha(t - t_o)} && t \geq t_o \\ &= 0 && t < t_o \end{aligned} \tag{86}$$

$$\begin{aligned} f_1(t - t_o) = h[-(t - t_o)] &= \alpha e^{-\alpha(t_o - t)} && t \leq t_o \\ &= 0 && t > t_o \end{aligned} \tag{87}$$

The value of K in Equation 79 is

$$K = \frac{1}{\int_{-\infty}^{\infty} f_1^2(t - t_o)\,dt} = \frac{1}{\int_{-\infty}^{t_o} \alpha^2 e^{2\alpha(t-t_o)}\,dt} = \frac{2}{\alpha} \tag{88}$$

Substituting $\frac{2}{\alpha}$ for K in Equation 79 gives

$$p(\omega_o, t_o) = \frac{1}{\pi\alpha} E_o(\omega_1, t_o) \tag{89}$$

Figures 13(a) and (b) are sketches of $f_1(t - t_o)$ and $|F_1(\omega)|$, the associated time and frequency windows used in the process.

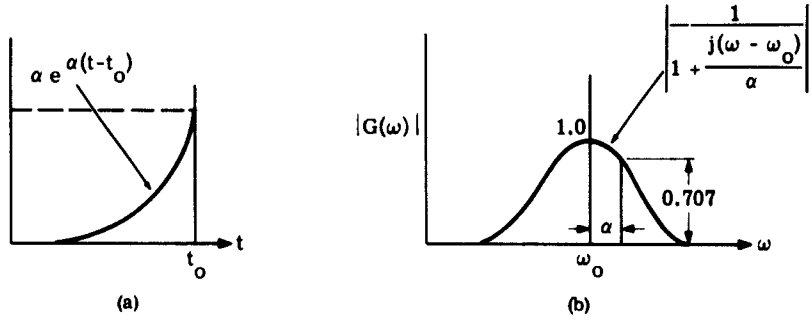

FIGURE 13. ASSOCIATED TIME AND FREQUENCY APERTURES. (a) Exponential time aperture. (b) Frequency aperture or filter function.

The time aperture is an exponential which gives greatest weight to the characteristics of f(t) at $t = t_o$, with the weight decreasing exponentially as $t_o - t$ becomes larger.

Substituting Equations 87 and 88 into Equation 70 gives

$$p(\omega_o, t_o) = \frac{\alpha}{\pi}\left\{\left[\int_{-\infty}^{t_o} e^{\alpha(t-t_o)} f(t) \cos \omega_o t\,dt\right]^2 + \left[\int_{-\infty}^{t_o} e^{\alpha(t-t_o)} f(t) \sin \omega_o t\,dt\right]^2\right\} \tag{90}$$

which is the expression used for evaluating $p(\omega_o, t_o)$ when first order low-pass filters are used for filters A and B of Figure 10.

Since the various frequency components of seismic surface waves propagate at different velocities, the initial part of the received wave will contain only those frequency components which propagate at the higher velocities, and the more slowly propagating frequencies will arrive later. Measurement of this dispersion of the arrival times for the different frequency components is an important part of analyzing the wave. The

exponential time aperture of Figure 13(a) is well suited for this type of work, since it gives major emphasis to the frequency characteristics of the portion of f(t) which is just entering the window.

An expression resembling Equation 90 has been defined as the e.m.p. (exponentially mapped past) power spectrum by Dr. Joseph Otterman [5]. The e.m.p. power spectrum is defined as follows:

$$p_\alpha(\omega) = \alpha^2\left[\int_{-\infty}^{t} f(x)e^{-\alpha(t-x)}\cos\omega(t-x)\,dx\right]^2 + \alpha^2\left[\int_{-\infty}^{t} f(x)e^{-\alpha(t-x)}\sin\omega(t-x)\,dx\right]^2 \tag{91}$$

In order to permit comparison of this expression with Equation 90, we show that cos ωx may be substituted for cos $\omega(t-x)$, and sin ωx may be substituted for sin $\omega(t-x)$ in Equation 91 without changing the value of $p_\alpha(\omega)$. Equation 91 can then be written in complex form:

$$\begin{aligned} p_\alpha(\omega) &= \alpha^2\left|\int_{-\infty}^{t} f(t)e^{-\alpha(t-x)}\cos\omega(t-x)\,dx + j\int_{-\infty}^{t} f(x)e^{-\alpha(t-x)}\sin\omega(t-x)\right|^2 \\ &= \alpha^2\left|\int_{-\infty}^{t} f(x)e^{-\alpha(t-x)}\left[\cos\omega(t-x) + j\sin\omega(t-x)\right]dx\right|^2 \\ &= \alpha^2\left|\int_{-\infty}^{\infty} f(x)e^{-\alpha(t-x)}e^{j\omega(t-x)}\,dx\right|^2 \\ &= \alpha^2\left|e^{j\omega t}\int_{-\infty}^{\infty} f(x)e^{-\alpha(t-x)}e^{-j\omega x}\,dx\right|^2 \end{aligned} \tag{92}$$

Since $\left|e^{j\omega t}\right| = 1$, this factor may be deleted from Equation 92 and we can write

$$p_\alpha(\omega) = \alpha^2\left|\int_{-\infty}^{t} f(x)e^{-\alpha(t-x)}e^{-j\omega x}\,dx\right|^2 = \alpha^2\left\{\left[\int_{-\infty}^{t} f(x)e^{-\alpha(t-x)}\cos\omega x\,dx\right]^2 + \left[\int_{-\infty}^{t} f(x)e^{-\alpha(t-x)}\sin\omega x\,dx\right]^2\right\} \tag{93}$$

Comparison of Equation 93 with Equation 90 reveals that since the corresponding integrals are identical,

$$p(\omega_o, t_o) = \frac{1}{\pi\alpha}\,p_\alpha(\omega) \tag{94}$$

where $p(\omega_o, t_o)$ is the time-varying power spectrum defined by Equation 90, and $p_\alpha(\omega)$ is the e.m.p. power spectrum defined by Equation 91.

Also, according to Equation 89

$$p(\omega_o, t_o) = \frac{1}{\pi\alpha} E_o(\omega_i, t_o) \tag{89}$$

and comparison of this with Equation 94 above shows that

$$E_o = p_\alpha(\omega) \tag{95}$$

Thus, the output voltage, E_o, of the analog-computer circuit directly represents the e.m.p. power spectrum as defined by Otterman, but this voltage must be multiplied by the factor $1/\pi\alpha$ to obtain the time-varying power spectrum defined by Equation 90.

We recall from the discussion following Equation 30 that the derivation of $p(\omega_o, t_o)$ is based on a power spectrum which includes negative as well as positive frequencies, and that

$$P(\omega_o, t_o) = 2p(\omega_o, t_o) \tag{96}$$

where $P(\omega_o, t_o)$ is the power density at ω_o for time t_o, and where the frequency spectrum of f(t) is considered to exist for positive values of ω only.

2.2.3.4. Change of Bandwidth with Frequency. When the analog-computer cicuit using first-order low-pass filters, as described in Section 2.2.3.3, is used for measuring the power or energy density at low frequencies such as 1 cps, the filter passband must be much narrower than 1 cps in order to give reasonable frequency resolution. At higher frequencies, such as 100 cps, this extremely narrow bandwidth is unsatisfactory because a large number of separate frequencies would have to be investigated to cover a given frequency range. Consequently, the filter bandwidth was changed for each interrogation frequency. It was experimentally determined that for seismic data, satisfactory frequency resolution could be obtained by making the filter bandwidth between the half-power points equal to 2.5% of the interrogation frequency ω_i. Thus, for the first-order low-pass filters,

$$\text{bandwidth} = 2\alpha = 0.025\omega_i \tag{97}$$

or solving for α,

$$\alpha = 0.0125\omega_i = 0.025\pi F_i \tag{98}$$

where $F_i = \omega_i/2\pi$

This value for α may be substituted in Equation 89 (repeated here),

$$p(\omega_o, t_o) = \frac{1}{\pi\alpha} E_o(\omega_i, t_o) \tag{89}$$

to give

$$p(\omega_o, t_o) = \frac{1}{0.025\pi^2 F_i} E_o(F_i, t_o) = \frac{40}{\pi^2 F_i} E_o(F_i, t_o) \tag{99}$$

Equation 99 is valid only when the bandwidth 2α is programmed to be 2.5% of the interrogation angular frequency ω_i.

Under these conditions, the frequencies to be investigated were chosen 0.01 decade apart, thus giving 200 separate interrogation frequencies in the two-decade range from 1 cps to 100 cps. With a 0.01-decade separation, the relationship between two adjacent interrogation frequencies is

$$\log \omega_{n+1} = \log \omega_n + 0.01 \tag{100}$$

Solving this for $\frac{\omega_{n+1}}{\omega_n}$ gives

$$\frac{\omega_{n+1}}{\omega_n} = 10^{0.01} = 1.0233 \tag{101}$$

Thus, the increase from any given interrogation frequency to the next higher is 2.33%, and since the bandwidth at each interrogation frequency is 2.5%, the frequency spectrum will be adequately covered, with no gaps between adjacent interrogation frequencies.

If only positive frequencies are considered as making up the seismic signal, then Equation 99 must be multiplied by two.

Combining Equations 96 and 99,

$$P(\omega_o, t_o) = 2p(\omega_o, t_o) = \frac{80}{\pi^2 F_i} E_o(F_i, t_o) \tag{102}$$

or, since $\omega_o = \omega_i$ and $\omega_i = 2\pi F_i$, P is also a function of F_i and t_o, and

$$P(F_i, t_o) = \frac{80}{\pi^2 F_i} E_o(F_i, t_o) \tag{103}$$

2.2.3.5. Computation of the Energy-Density Spectrum. If the output of the adder of Figure 10 is integrated, the result is

$$E_7 = \int_0^{t_o} E_o\, dt = \pi\alpha \int_0^{t_o} p(\omega_o, t_o)\, dt = \frac{\pi\alpha}{2} \int P(\omega_o, t_o)\, dt \tag{104}$$

And, since the energy density W_d is given by

$$W_d(\omega_o, t_o) = \int_0^{t_o} P(\omega_o, t_o)\,dt \tag{105}$$

(assuming $f(t) = 0$ for $t < 0$)

$$E_7 = \frac{\pi\alpha}{2} W_d(\omega_o, t_o)\,dt \tag{106}$$

If we substitute $0.025\pi F_i$ for α and designate E_7 and W_d as functions of the two variables, F_i and t_o, we obtain

$$W_d(F_i, t_o) = \frac{80}{\pi^2 F_i} E_7(F_i, t_o) \tag{108}$$

3
RESULTS

Since the time-varying power-density spectrum $P(F_i, t_o)$, discussed in Section 2, is a function of the two variables F_i and t_o, there are two basic ways in which this data could be plotted. Frequency, F_i, could be held constant and the power density P could be plotted as a function of time t_o; or plots could be made of power density versus frequency for various fixed values of time.

Figure 14(a) is an illustration of the first type of plot, applied to a seismometer signal produced by an earthquake. These curves, with the exception of the bottom one, show the product power density and frequency at various frequencies as a function of time. The bottom curve is a plot of instantaneous power versus time for the signal being analyzed, and is included to serve as a time reference. Note that although signals were received immediately after the sixth second, according to the bottom curve, the individual curves for the various frequencies from 0.5 cps to 1.41 cps show no significant activity before the ninth second. Figures 14(b)(c)(d) and (e) are continuations of Figure 14(a) for increasingly higher interrogation frequencies. As the frequency becomes higher, the starting time becomes earlier until it corresponds to the starting time of the seismic wave itself.

Another interesting phenomenon is the separation of the trace into two separate parts, one starting at 6 seconds and the other at about 20 seconds, for frequencies above 7 cps.

The second method of presenting data (i.e., power density versus frequency for fixed values of time) was slightly modified by making the ordinate the product of energy density and frequency instead of power density.

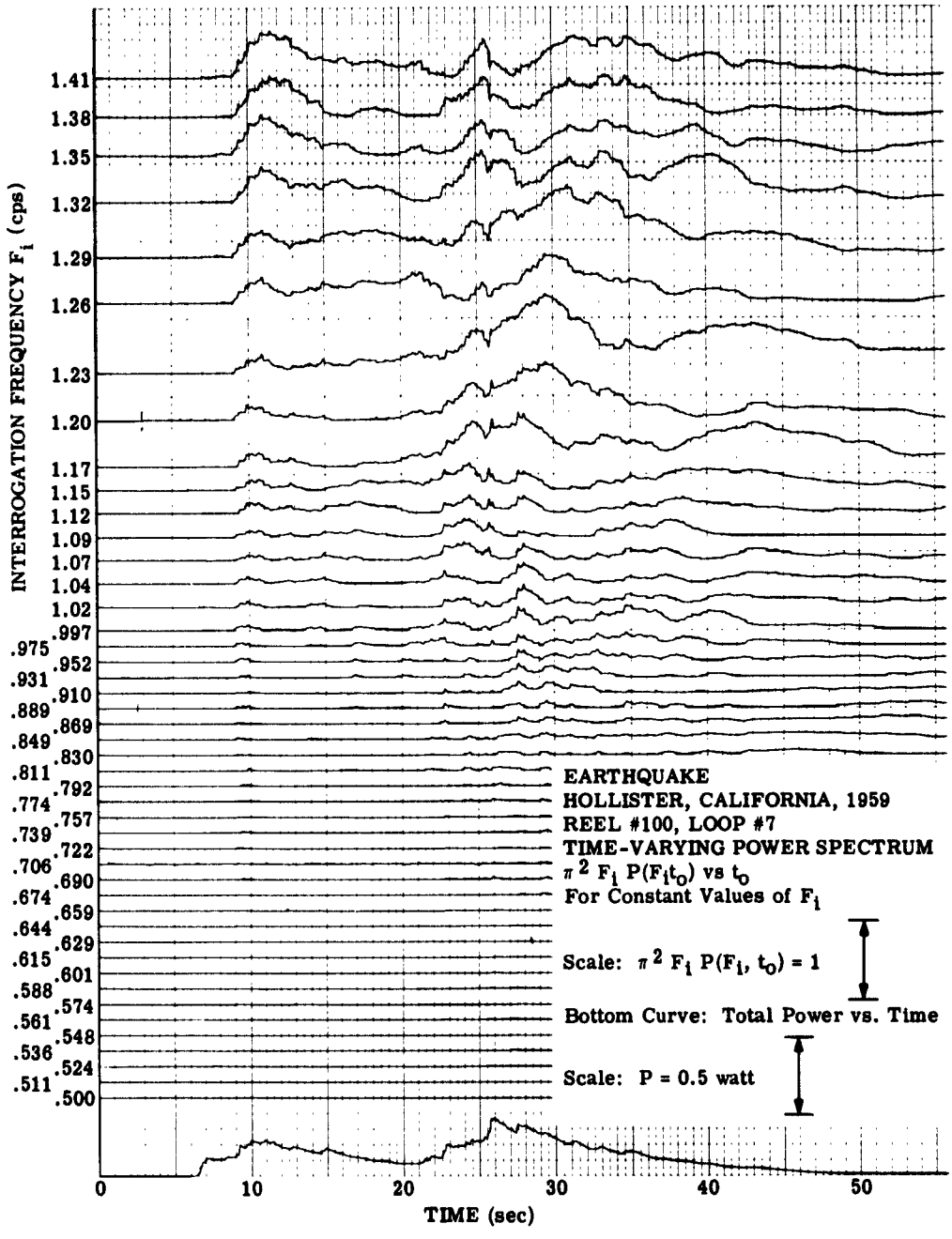

FIGURE 14. CURVES OF POWER DENSITY VERSUS TIME FOR CONSTANT F_i. (a) 0.5 to 1.41 cps.

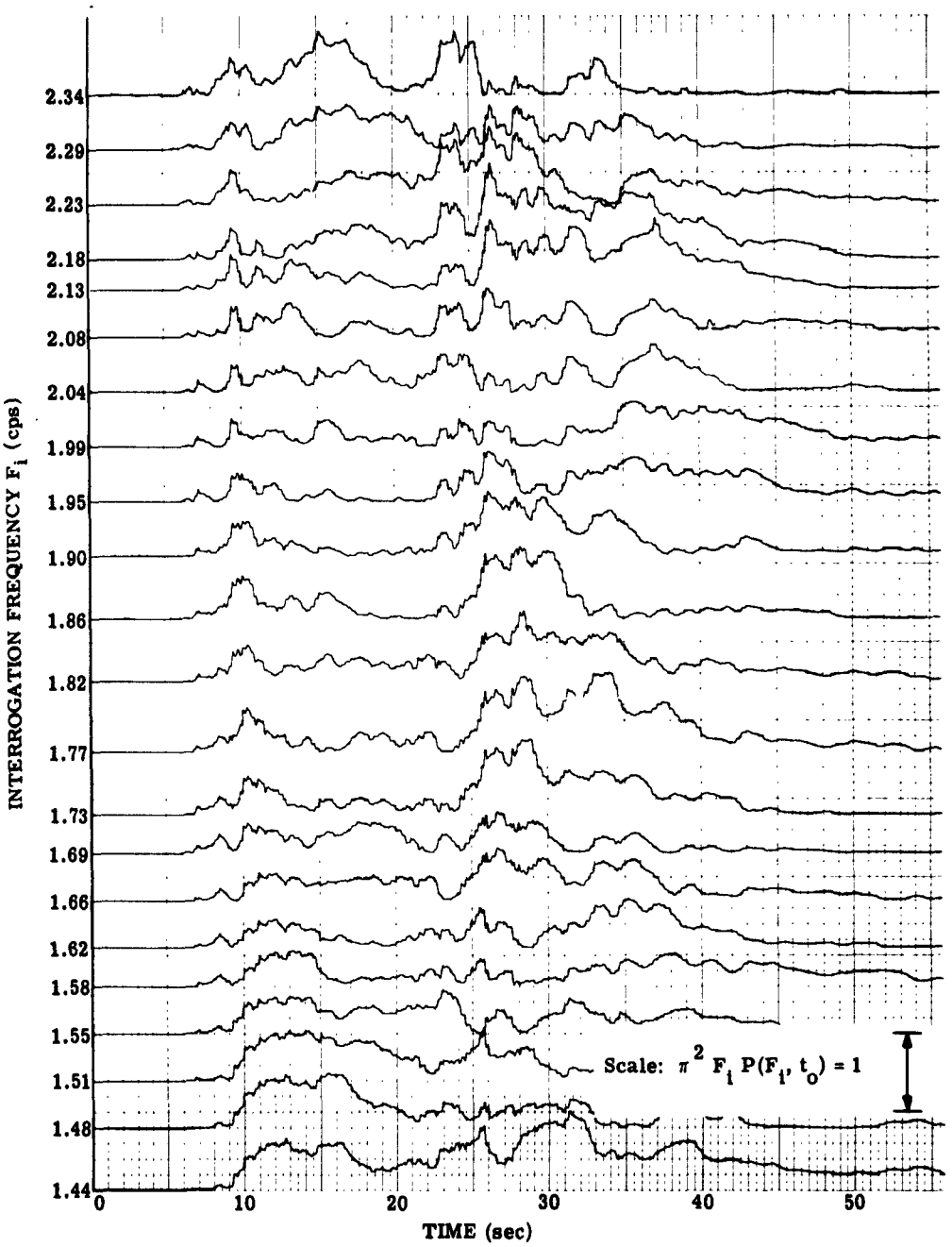

FIGURE 14 (Continued). (b) 1.44 to 2.34 cps.

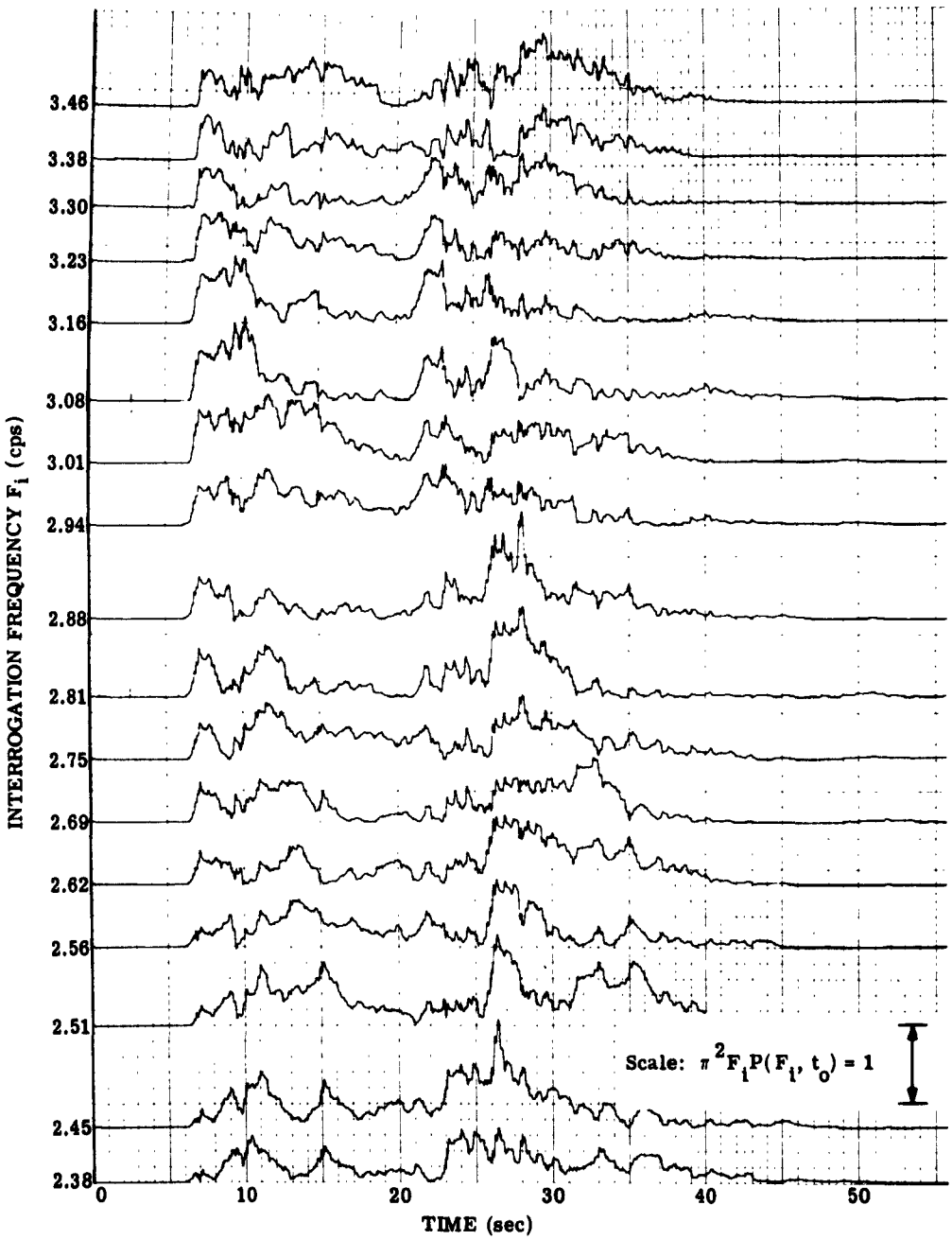

FIGURE 14 (Continued). (c) 2.39 to 3.46 cps.

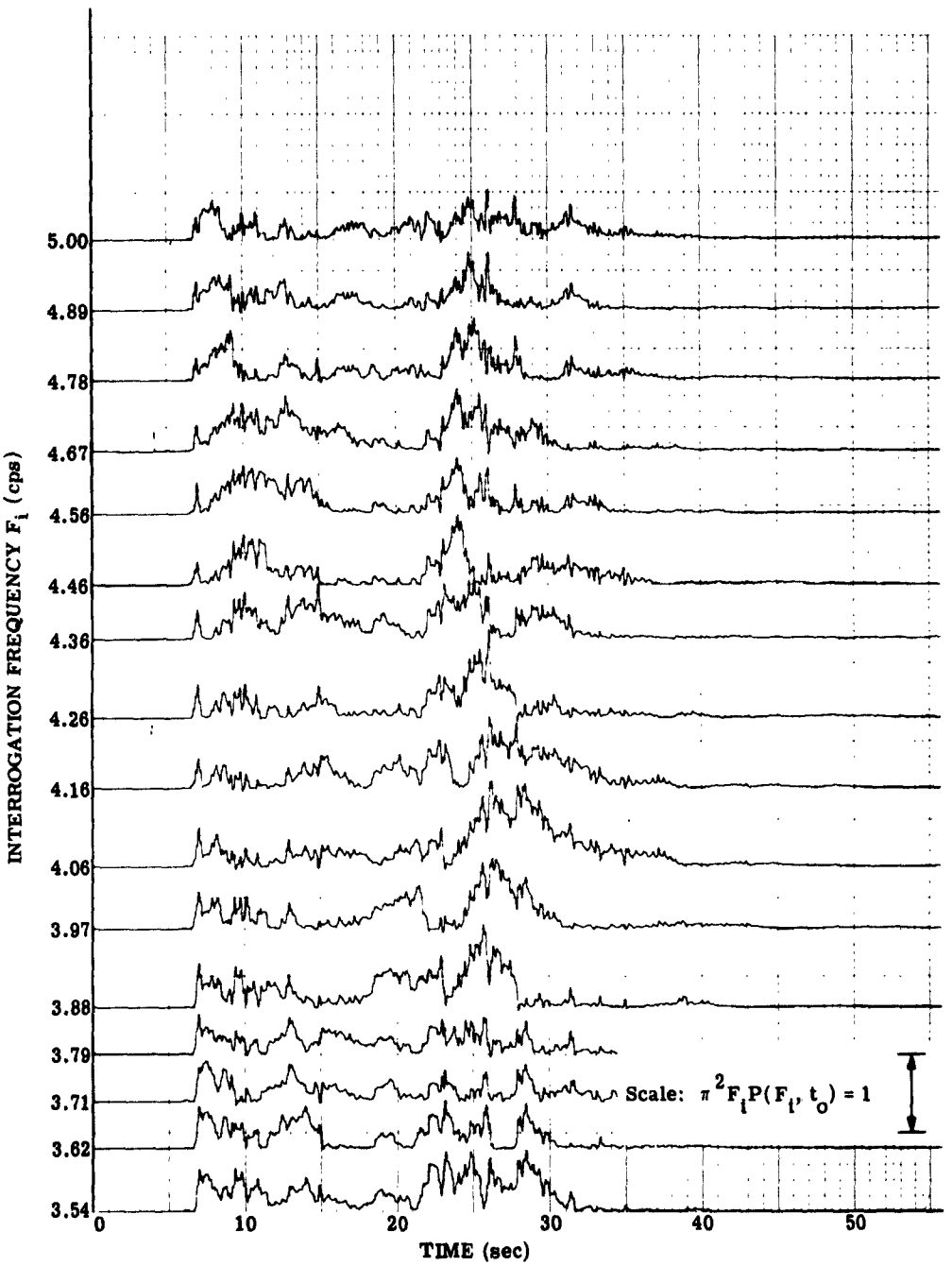

FIGURE 14 (Continued). (d) 3.54 to 5.00 cps.

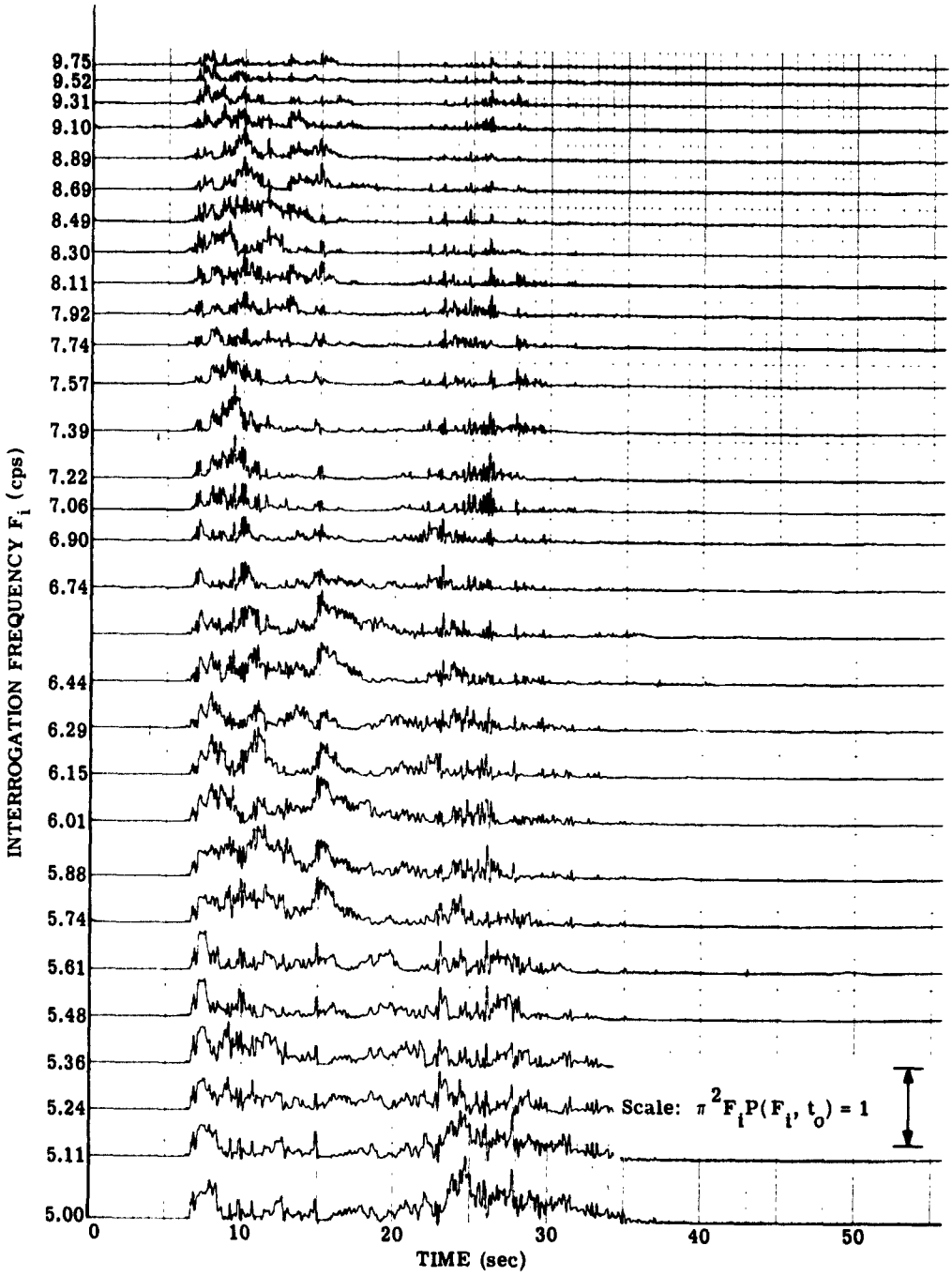

FIGURE 14 (Continued). (e) 5.00 to 9.75 cps.

Results of this type are shown in Figure 15. The curves labeled 1 through 5 represent the signal's total energy-density-frequency product, as a function of frequency, for times of 11, 22, 33, 44, and 55 seconds from "zero" time shown on Figure 14. Thus, curve 1 represents frequency-energy-density product as a function of frequency, for the first 11 seconds of the signal; curve 2 is for the first 22 seconds, and so on. Finally, curve 5 shows the frequency-energy-density product versus frequency for the entire seismic signal. The separation between the curves at any specific frequency is proportional to the average power density for the time interval bounded by the two curves. A logarithmic frequency scale was used for Figure 15 in order to give uniform separation between the separate interrogation frequencies, which are spaced 0.01 decade apart. (See Section 2.2.3.4.)

It can be readily shown that if the curves of Figure 15 are extended to cover all frequencies from 0 to ∞, the area under the highest curve (number 5) is proportional to the total energy of the seismometer signal. The area under the curve is given by

$$A = \int_{-\infty}^{\infty} y\,dx \tag{109}$$

For Figure 15,

$$y = K_1 F_i W_d \tag{110}$$

where K is a scaling constant, F is the frequency, and W_d is the energy-density spectrum in watt-seconds per radian per second. Also for Figure 15,

$$X = K_2 \log_{10} F = \frac{K_2}{\log_e 10} \log_e F \tag{111}$$

and

$$dx = \frac{K_2}{\log_e 10} \frac{dF}{F} \tag{112}$$

Substituting into Equation 109,

$$A = \frac{K_1 K_2}{\log_e 10} \int_0^{\infty} W_d\,dF \tag{113}$$

but the total energy in the signal, by the Fourier integral energy theorem, is

$$W = \int_0^{\infty} W_d\,d\omega = 2\pi \int_0^{\infty} W_d\,dF \tag{114}$$

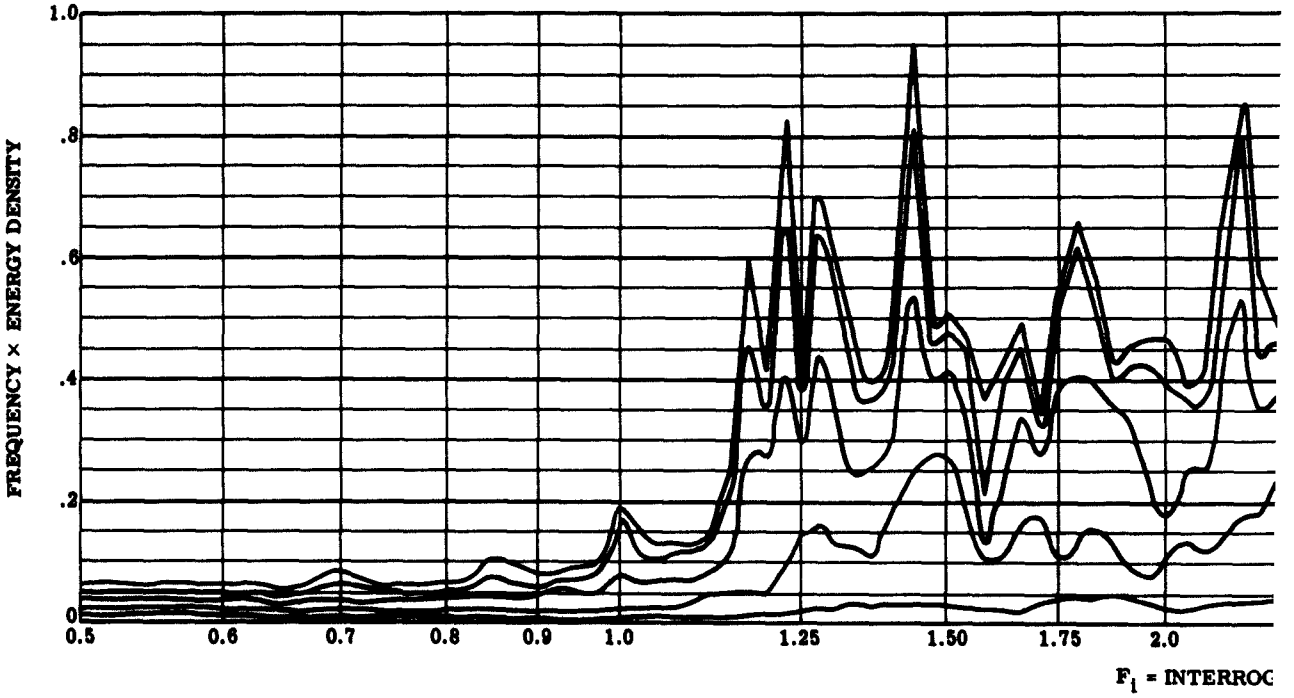
FREQUENCY × ENERGY DENSITY
1.0
.8
.6
.4
.2
0
0.5
0.6
0.7
0.8
0.9
1.0
1.25
1.50
1.75
2.0
F1 = INTERROG

FIGURE 15. EN

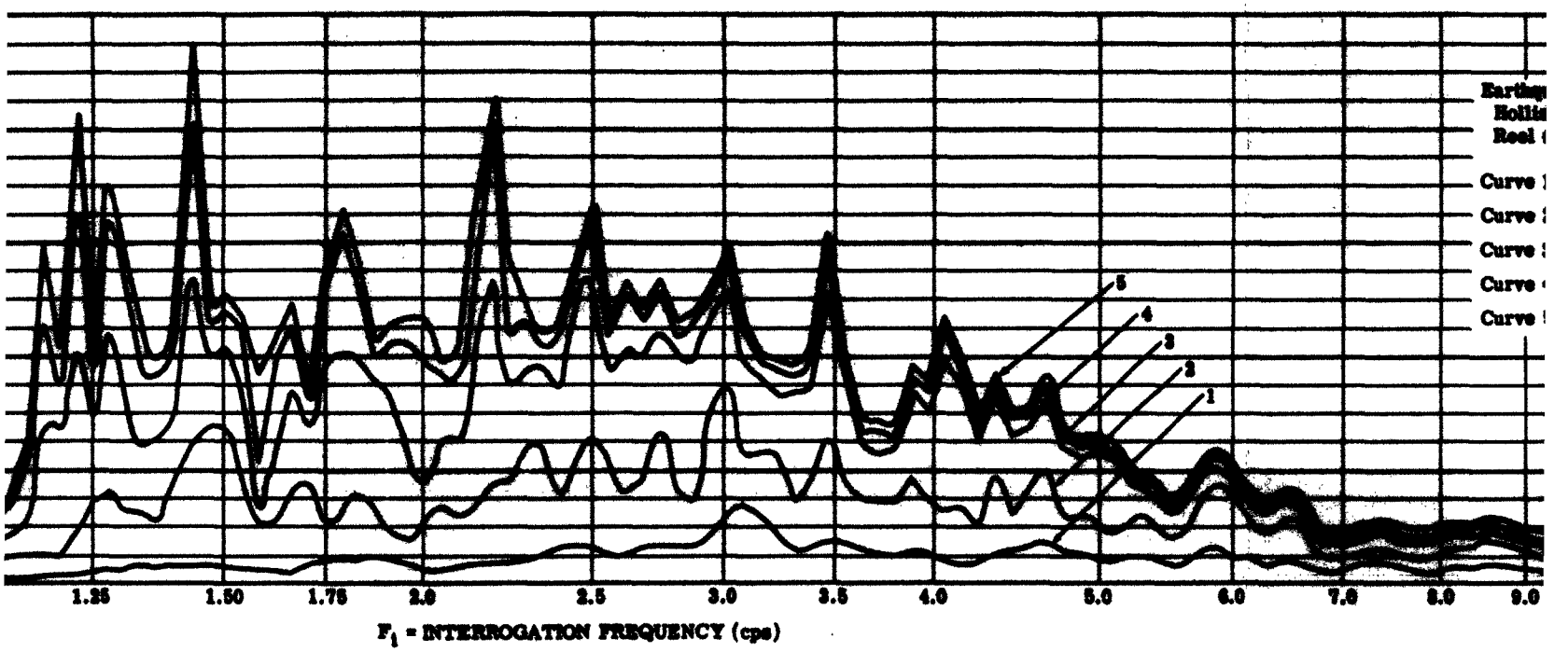

FIGURE 16. ENERGY-DENSITY BANDWIDTH VERSUS FREQUENCY

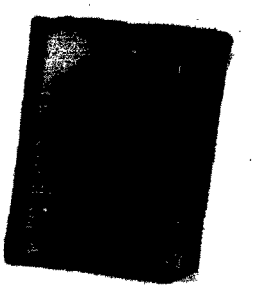

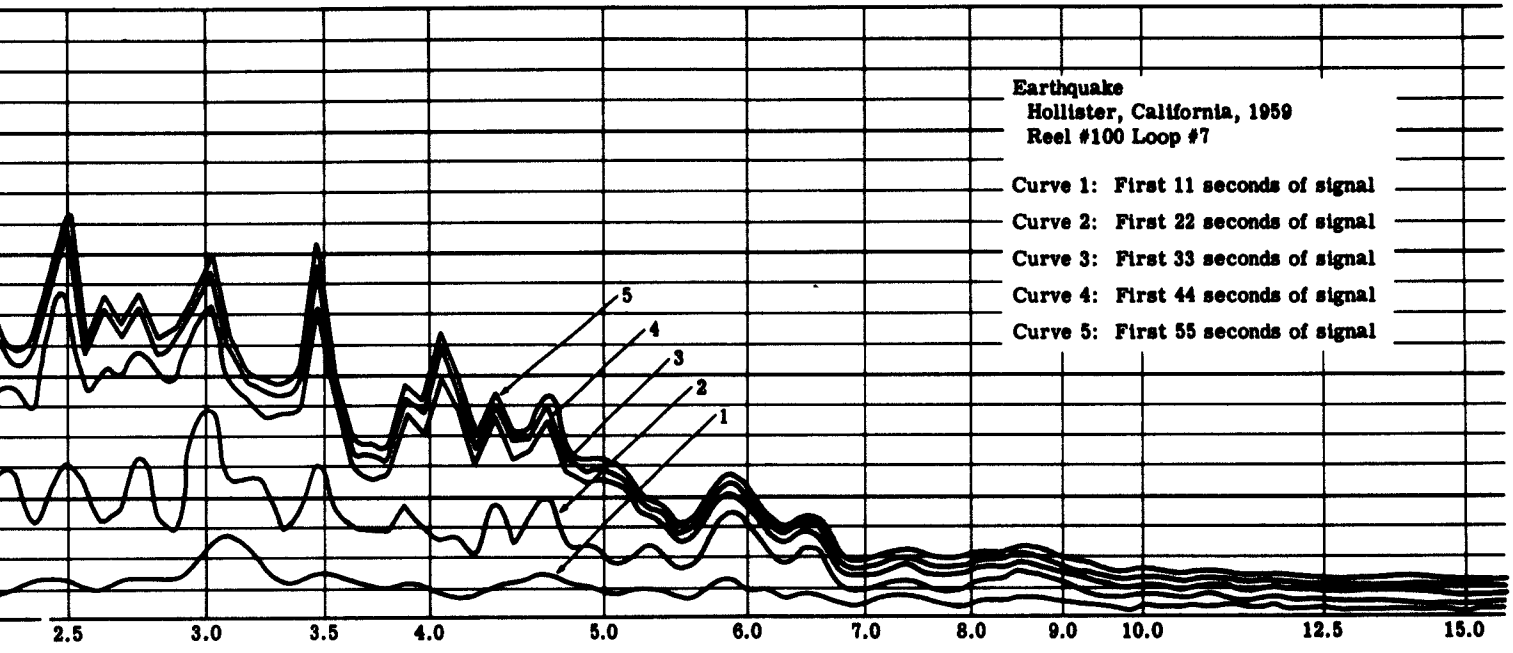

ATION FREQUENCY (cps)

ERGY-DENSITY BANDWIDTH VERSUS FREQUENCY

and, from Equation 113,

$$\int_0^\infty W_d dF = \frac{A \log_e 10}{K_1 K_2} \tag{115}$$

Therefore,

$$W = \frac{2\pi \log_e 10}{K_1 K_2} A = K_3 A \tag{116}$$

Thus, aside from the fact that FW_d is readily available from the computer circuit, plotting this quantity versus log F instead of W_d versus log F has the additional advantage that the area under the curve is proportional to total energy. (This would also be true for a plot of W_d versus F, but would not be true for W_d versus log F.)

It is clear that the area under any one of the curves of Figure 15 is proportional to the total energy of the signal up to the time represented by that curve. The curves of Figures 14 and 15 represent specific results for a particular seismic wave. During the investigation, about 45 separate tape-recorded seismic records were processed in the manner indicated. A detailed discussion of the seismologically significant results of this investigation is being deferred to a later report, since the present report is concerned with theory and techniques only.

4
CONCLUSIONS AND RECOMMENDATIONS

4.1. CONCLUSIONS

(a) For obtaining useful information from a frequency analysis of a seismic signal, the formal methods which analyze the entire signal in terms of constant-amplitude sinusoids of various frequencies are unsatisfactory. Instead, some method which leads to a "time-varying" spectrum must be used.

(b) Any "time-varying" spectrum so obtained necessarily involves some approximations, since any analysis of a signal in terms of amplitude-modulated sinusoidal waveforms is not unique, but depends upon the characteristics of the filter or time window used.

(c) In obtaining a time-varying power spectrum by any technique, the time resolution and frequency resolution are interrelated in such a manner that an improvement in one results in a degradation of the other. They can both be improved somewhat by optimum choice of time and frequency apertures, but the basic problem arises from the interrelated nature of the time and frequency domains, and not from equipment limitations.

(d) Three possible techniques for obtaining a time-varying power spectrum are:

1. Weighted Fourier analysis, using a moving "time window" as the weighting function.
2. Use of variable filters or "frequency apertures" and measuring the amount of power, as a function of time, which passes through the filter for various frequencies.
3. Translation of the frequency spectrum of the seismic wave by heterodyning techniques in such a manner that each portion of the spectrum in turn may be passed through a fixed-frequency filter.

Theoretically, these three techniques are equivalent, and no one method can give results which are superior to those obtained from the others. Choice of the technique to be used should be based on available equipment and its limitations.

(e) Although it offers no theoretical advantage over methods using filters, the analog computing technique described in this report is by its flexibility probably is the most satisfactory for developing and testing various methods. After an optimum method of analyzing seismic data has been found, it would probably be advantageous to build special apparatus for routine analysis rather than continue using an analog computer. Such apparatus would probably be less expensive to operate and would perform the analysis much more rapidly than the analog computer setup.

(f) Seismic spectra in general are not smooth, but contain a number of definite peaks. In order to resolve these peaks, a filter bandpass of about 2 1/2% of the center frequency appears necessary. No significant improvement in resolution is obtained by using narrower filters.

4.2. RECOMMENDATIONS

Recommendations for future work may be divided into two categories: (a) optimization of frequency-analysis techniques; and (b) development of other methods of analyzing seismic data. The principal object of future investigation would be to develop methods of analyzing seismic waves which lead to accurate determination of the nature and location of the sources and the physical characteristics of the transmission path. Investigation of the spectral characteristics of a seismic wave is only one of several reseach programs which may lead to significant results.

4.2.1. FURTHER DEVELOPMENT AND REFINEMENT OF FREQUENCY-ANALYSIS TECHNIQUES. We recommend that further research be performed on the items below.

(a) Theoretical and experimental investigations to find a technique which gives the best compromise between time and frequency resolution when applied to seismic data.

(Although the time and frequency apertures may not be independently chosen since the choice of one automatically specifies the other, it seems possible to find a system which gives optimum results in terms of time resolution and frequency resolution considered simultaneously. A particular frequency aperture to

be tested is one with a shape corresponding to the bell-shaped Gaussian distribution curve. Since the Fourier transform of this curve is also a Gaussian distribution curve, the time aperture in this case would be identical in shape with the frequency aperture.)

(b) Attempting to find a graphical presentation type of a time-varying spectrum which will result in a "signature" characteristic of the type of seismic wave being analyzed.

(c) Investigating the possibility of accurately measuring the arrival times of the principal frequency components of the seismic wave by first using a narrow filter to determine the center frequencies of peaks in the spectrum, and then using wideband filters to measure the arrival time of these frequencies.

(d) Investigating the feasibility of playing the tape-recorded seismic signal both forward and backward to measure more accurately the arrival time of each frequency component.

4.2.2. DEVELOPMENT OF METHODS OTHER THAN FREQUENCY ANALYSIS FOR ANALYZING SEISMIC DATA. Other methods of analysis which could be investigated are the method of time-varying autocorrelation functions and that of time-varying amplitude-distribution functions.

(a) The autocorrelation function of a function of time is useful not only in power-spectra determination, but also in detecting periodic signals. Any periodic signals which were concealed in seismic data would probably appear only during certain time intervals. Thus, techniques for determining a time-varying autocorrelation function could be developed and applied to seismic data.

(b) A signal which has uniform statistical characteristics for any interval of time (stationary function) is often described in terms of its amplitude-distribution function. Since the statistical characteristics of a seismic wave are not uniform in time, the amplitude-distribution function as measured for one time interval may be considerably different from that determined for the preceding or following time interval. Analog computing techniques similar to those used for time-varying power-spectra measurement could be used to determine a time-varying amplitude-distribution function. Whether or not such a function would be useful for describing seismic signals in terms of their source and transmission path would be determined experimentally.

Appendix A
SEISMIC-SIGNAL CORRECTION

In the following, the notation f(t) designates a signal produced by a seismometer with a flat response, and f'(t) represents the output of a seismometer which is sensing the signal. In general, f'(t) differs from f(t) in the seismometer's response characteristics. The seismometer output, f'(t), had been recorded on magnetic tape, using an FM recording system, and the analysis was performed on the signal played back from the tape. No significant frequency distortion resulted from the tape-recording and reproducing processes, but a slight difference between the center frequency of the playback demodulator and the carrier frequency of the recorded signal generated a d-c bias voltage which was not originally present at the seismometer output. In order to obtain an accurate reproduction of f(t) for frequency analysis, both the d-c introduced by the record-reproduce process, and the spectral distortion introduced by the seismometer response were removed.

If the complex frequency spectrum of f(t) is F(s), and the seismometer response is G(s), the output of the seismometer is given by

$$F'(s) = F(s)G(s) \tag{117}$$

Since the record-reproduce process adds a d-c bias, the output of the playback demodulator is given by

$$F''(s) = F'(s) + \text{bias} = F(s)G(s) + \text{bias} \tag{118}$$

Equation 118 can be solved for F(s) to give

$$F(s) = \frac{F''(s) - \text{bias}}{G(s)} \tag{119}$$

and the time response corresponding to F(s) then represents f(t).

The recording process is illustrated by the upper block diagram of Figure 16. The lower block diagram of this figure illustrates the arrangements of the correcting filters in the playback setup. The FM signal from the tape-playback unit enters the demodulator, where it is converted to a signal corresponding to F'(s) or f'(t). The filter block with the transfer characteristic $\frac{s\tau}{1 + s\tau}$ removes any d-c bias from the output of the demodulator, and the block labeled 1/G(s) removes the effect of the seismometer response from the signal. The output of the inverse seismometer circuit is then approximately f(t), the error depending upon how accurately the inverse seismometer response is represented by the 1/G(s) block.

Average frequency-response characteristics of two types of seismometers (Benioff and Willmore) are shown in Figure 17. These curves represent the average of a number of curves obtained from shaketable

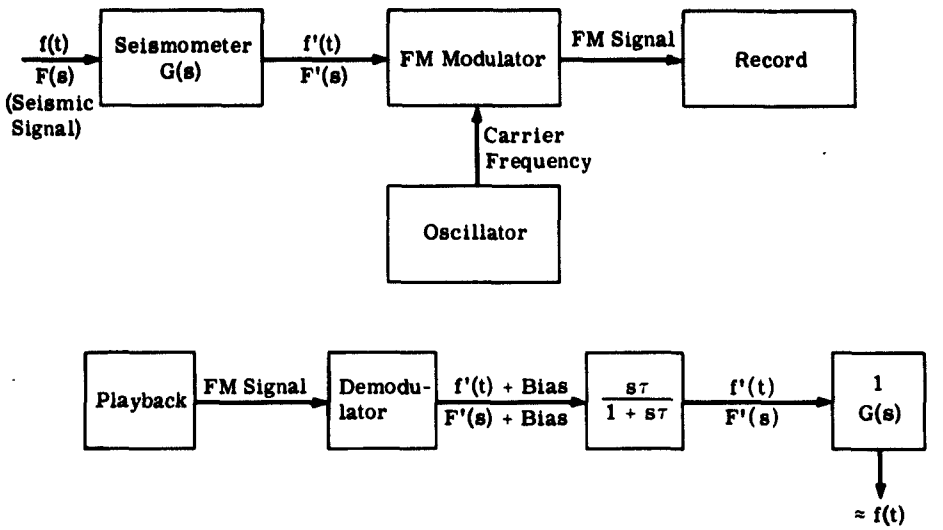

FIGURE 16. SEISMIC-SIGNAL RECORDING AND PLAYBACK

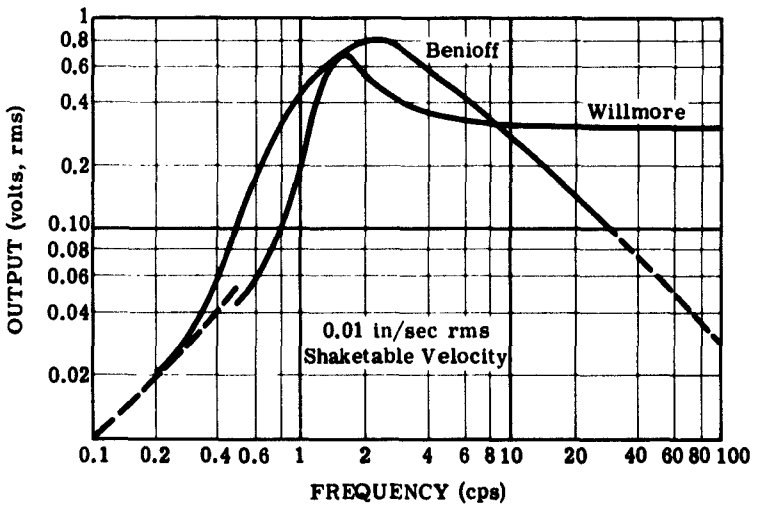

FIGURE 17. SEISMOMETER RESPONSE

tests. For these tests, the input signal, as obtained from the shaketable, was a sinusoid having an rms velocity of 0.01 inches per second. The curves show the resulting rms voltage output of the seismometers as a function of frequency. In Figure 17, the peak response of the Benioff curve is about 0.8 volt at 2.2 cps. If the inverse seismometer response filter had a gain of unity at this frequency, the voltage scaling from the seismometer-filter combination would be 0.8 volt per inch per second. If the correcting filter has a gain of 1/0.8 at this point, however, the output scaling of the seismometer-corrector combination is 1 volt per inch per second over the frequency range for which the corrections are valid.

A.1. BENIOFF-SEISMOMETER RESPONSE CORRECTION

The response curve for the Benioff seismometer is redrawn in Figure 18. Below it a frequency-response curve is plotted as measured from an analog-computer mechanization which was used to approximate the inverse seismometer response.

The resultant frequency response of the seismometer-filter combination is the product of the two curves; it is also plotted in Figure 18.

As shown, the resultant droops at both the high- and low-frequency ends, but since the range of the investigation was from 0.5 to 50 cps, with the major portion of the return well within these limits, it was felt that this droop was permissible.

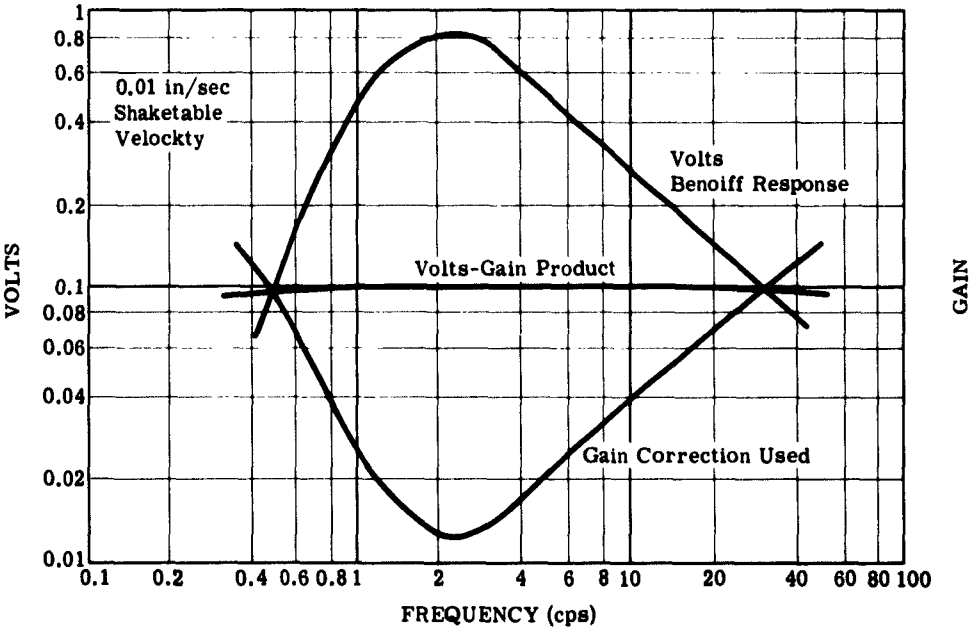

FIGURE 18. BENIOFF-SEISMOMETER CORRECTION CURVES

The transfer function G(s) between the velocity of the shaketable and the output of the Benioff seismometer is approximated by

$$G(s) \approx \frac{Ks}{\frac{s^2}{\omega_n^2} + \frac{2\zeta}{\omega_n} s + 1} \tag{120}$$

where K = a gain constant

ω_n = the natural angular frequency

ζ = a damping factor

The inverse of this function is

$$\frac{1}{G(s)} = \frac{1}{K}\left(\frac{s}{\omega_n^2} + \frac{2\zeta}{\omega_n} + \frac{1}{s}\right) \tag{121}$$

In order to avoid difficulties arising from differentiating high-frequency noise and from integrating low-frequency drift, the transfer function for the inverse response was changed to

$$\frac{1}{G(s)} \approx \frac{1}{K}\left(\frac{\tau_2 s}{\omega_n^2(1+\tau_2 s)} + \frac{2\zeta}{\omega_n} + \frac{1}{\tau_1 s + 1}\right) \tag{122}$$

The mechanization of $\frac{1}{\tau_1 s + 1}$ is an approximate integrator which is good for frequencies much greater than $1/\tau_1$ radians per second, and the mechanization of $\frac{\tau_2 s}{1+\tau_2 s}$ is an approximate differentiator which is valid for frequencies much less than $1/\tau_2$ radians per second. Rearranging terms of Equation 122 in order of ascending "break-point" frequencies of the approximate integrator and the approximate differentiator gives

$$\frac{1}{G(s)} \approx \frac{1}{K}\left[\frac{1}{\tau_1 s + 1} + \frac{2\zeta}{\omega_n} + \frac{\tau_2 s}{\omega_n^2(1+\tau_2 s)}\right] \tag{123}$$

Figures 19(a) and 19(b) show the response curves that would result if perfect integrators and differentiators were used to generate the inverse Benioff response characteristics called for in Equation 121. Here the response curve would start with a gain of infinity for d-c (curve a) and follow a negative integrator slope down with increasing frequency until it met the added positive slope (curve b) of the differentiator, where the gain would rise again back to infinity for infinite frequency. The constant term of Equation 121 adds to the gain value and, at the point of intersection of the negative and positive gain slopes, adjusts the value and shape of the minimum gain area. Figures 19(c) and 19(d) show the response curves of an approximate integrator and differentiator which are specified by Equation 123. From inspection of Figures 19(c) and 19(d), it is apparent that the break-point frequencies must be moved up the slopes as far as possible so that the

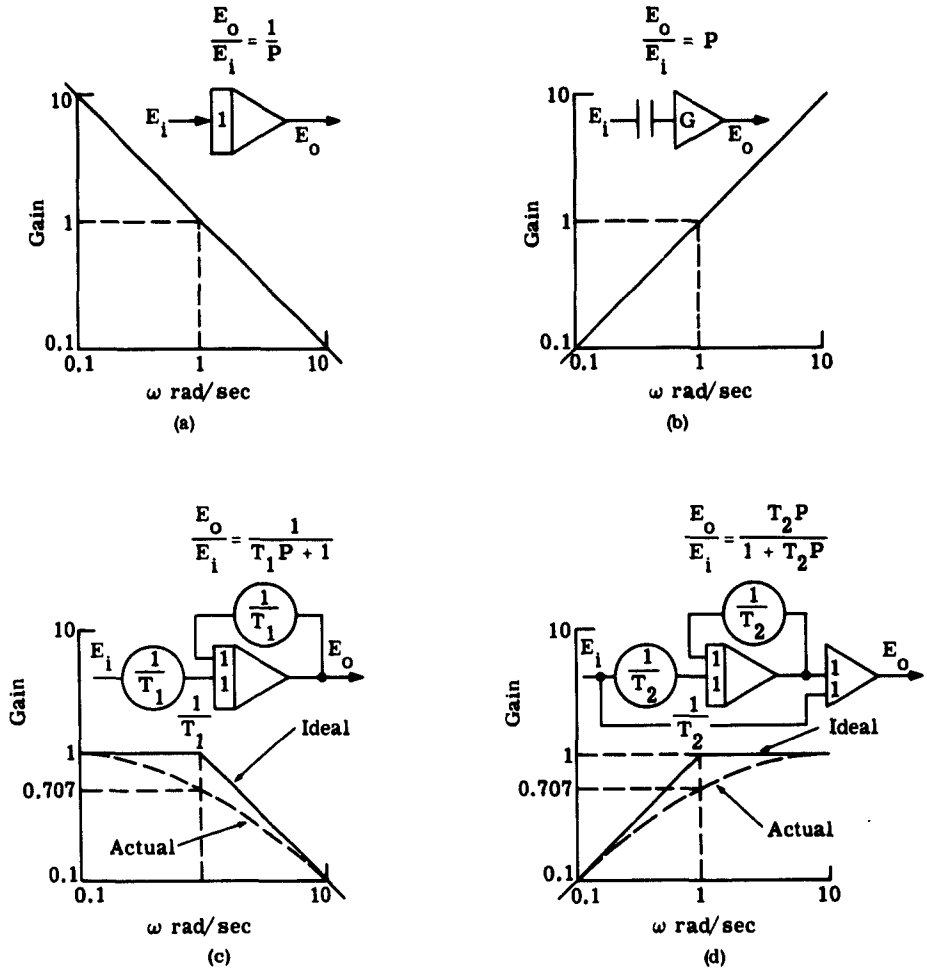

FIGURE 19. RESPONSE CURVES OF ACTUAL AND APPROXIMATE INTEGRATORS AND DIFFERENTIATORS. (a) Integrator. (b) Differentiator. (c) Approximate integrator. (d) Approximate differentiator.

actual curve closely matches the ideal curve within the frequency range of interest. This was done and the inverse Benioff response curve was followed almost perfectly for all test frequencies used; but for the actual runs the high-frequency gain was too much for the electronic multiplier. If the frequency of the signal and/or noise is much above 100 cps, the amplitude must be greatly reduced in order to keep the electronic multiplier from overloading.

High-frequency response was suppressed enough to satisfy the requirements of the electronic multiplier by adding a small feedback capacitor around the output amplifier of the inverse filter, as shown in Figure 20. In order to shorten the time constant of the d-c bias eliminator (an approximate differentiator), its break frequency was moved up, which made the addition of another approximate integrator necessary to increase the negative slope at the low-frequency end of the inverse Benioff filter. The completed filter had a frequency-response curve which accurately approximated the inverse Benioff response characteristics within the frequency range of interest, and which dropped off rapidly for frequencies outside this range.

Figure 20 shows an analog-computer diagram for the solution of the inverse Benioff response characteristic. The parts which were added to compensate for the analog computer limitations are drawn with dashed lines.

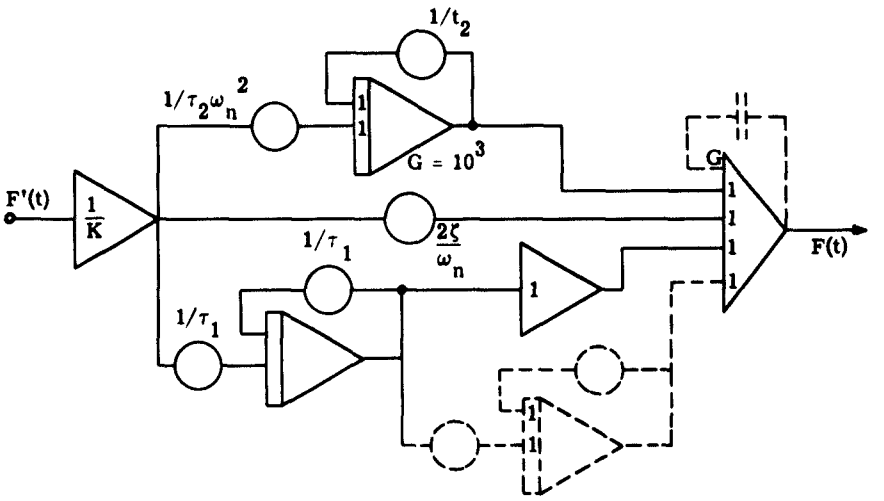

FIGURE 20. ANALOG-COMPUTER CIRCUIT FOR INVERSE BENIOFF-SEISMOMETER RESPONSE

A.2. WILLMORE-SEISMOMETER RESPONSE CORRECTION

The Willmore-seismometer response and the inverse response function used are shown in Figure 21. Since the gain at the high-frequency end is only about 3.3 for a maximum, no trouble was encountered in the solution.

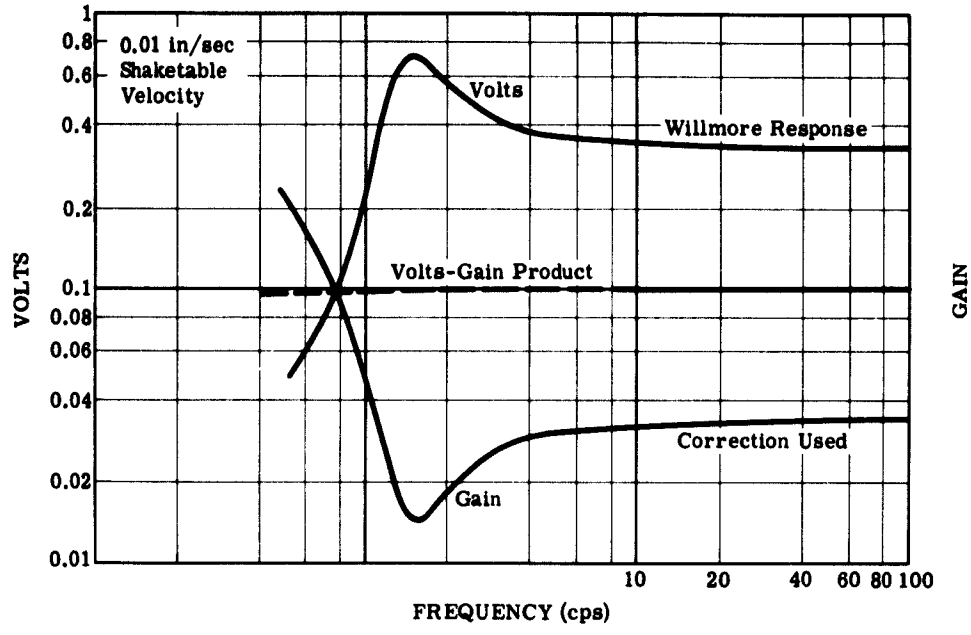

FIGURE 21. WILLMORE-SEISMOMETER CORRECTION CURVES

The transfer operator for the Willmore seismometer was approximated by

$$G_w(s) = \frac{K \frac{s^2}{\omega_n^2}}{\frac{s^2}{\omega_n^2} + \frac{2\zeta}{\omega_n} s + 1} \tag{124}$$

The inverse of this operator is

$$\frac{1}{G_w(s)} = \frac{1}{K} \left(\frac{\frac{s^2}{\omega_n^2} + \frac{2\zeta}{\omega_n} s + 1}{\frac{s^2}{\omega_n^2}} \right) \tag{125}$$

or

$$\frac{1}{K}\left(1+\frac{2\zeta\omega_n}{s}+\frac{\omega_n^2}{s^2}\right) \tag{126}$$

1/s is replaced here by the previously used expression $\frac{1}{\tau_1 s+1}$; thus the final equation is

$$\frac{1}{\text{response}}=\frac{1}{K}\left[\omega_n^2\left(\frac{1}{\tau_1 s+1}\right)^2+2\zeta\omega_n\left(\frac{1}{\tau_1 s+1}\right)+1\right] \tag{127}$$

The analog-computer circuit for this inverse response filter is shown in Figure 22.

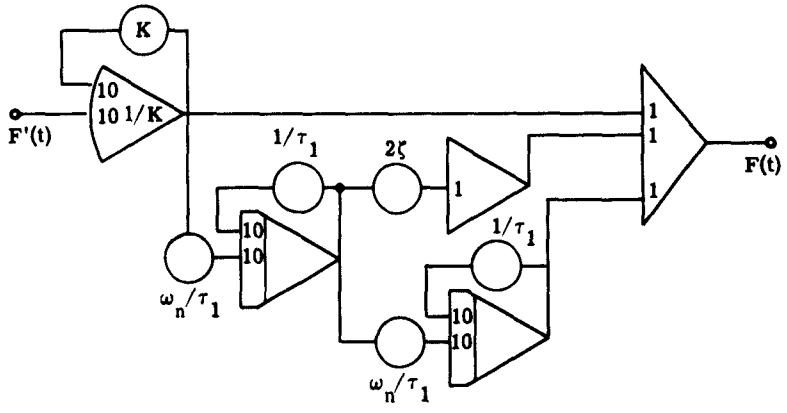

FIGURE 22. ANALOG-COMPUTER CIRCUIT FOR THE INVERSE WILLMORE-SEISMOMETER RESPONSE FILTER

Appendix B
ANALOG-COMPUTER IMPLEMENTATION

This appendix contains a more detailed description of the analog computing circuits than that presented in Section 2.2.3. of this report. The main computing circuits were assembled on a "PACE" computer made by Electronic Associates, Inc. The automatic programming was performed by additional conventional analog equipment built in the IST Analog Computer Laboratory. The interrogation frequency ω_1 for each run was selected by a digital-to-analog converter, operating from a punched-paper-tape reader.

B.1 ANALOG-COMPUTER ARRANGEMENT

Figure 23 is a block diagram of the complete analog-computer setup used for the frequency analysis of seismic signals. It consists of the basic computing block diagram of Figure 10 and the blocks used for correcting the recorded seismic signal, controlling the computer, and plotting the final results. Input information is received from two tape-recorder channels, shown at the upper left in Figure 23. Channel 1 is the control channel and channel 2 is the signal or information channel.

The signal from the demodulator for channel 2, the information channel, is f''(t). As explained in Appendix A, this signal consists of f(t) multiplied by the seismometer response and containing a small d-c bias. The bias eliminator is a high-pass filter which removes any d-c component from the signal. Its output is f'(t), the seismic signal f(t) multiplied by the seismometer response characteristics. Switches SW1 and SW2 may be positioned either to pass f'(t) directly into the computer circuits, or to insert the proper inverse seismometer filter and thus produce f(t), corresponding to the output of a seismometer with a flat response.

The corrected signal f(t) then enters the basic computing circuit, whose operation has been explained qualitatively in Section 2.2.3. In order to explain the operating sequence and at the same time quantify the results somewhat, we assume that the signal f(t) is replaced by a sinusoid A sin ωt. Then, the block marked "Multiplier A" in the upper channel multiplies the signal A sin ωt by cos $\omega_1 t$ from the oscillator block to produce at its output

$$E_1 = A \sin \omega t \cos \omega_1 t$$

or

$$E_1 = \frac{A}{2} [\sin (\omega - \omega_1)t + \sin (\omega + \omega_1)t]$$

and multiplier B in the lower channel multiplies the signal A sin ωt by sin $\omega_1 t$ from the oscillator to produce at its output

$$E_2 = \frac{A}{2} [\cos (\omega - \omega_1)t + \cos (\omega + \omega_1)t]$$

Filter A in the upper channel and filter B in the lower channel are both low-pass filters and, as such, attenuate all signals except those of zero frequency. Consequently, the sum-frequency terms [sin $(\omega + \omega_1)t$ and cos $(\omega + \omega_1)t$] in the above equations are attenuated to such a degree that their amplitudes may be considered negligible at the outputs of the filters. Thus, the output of filter A of the upper channel is

$$E_3 = \frac{A}{2} \sin (\omega - \omega_1)t \; G(\omega - \omega_1)$$

and the output of filter B of the lower channel is

$$E_4 = \frac{A}{2} \cos (\omega - \omega_1)t \; G(\omega - \omega_1)$$

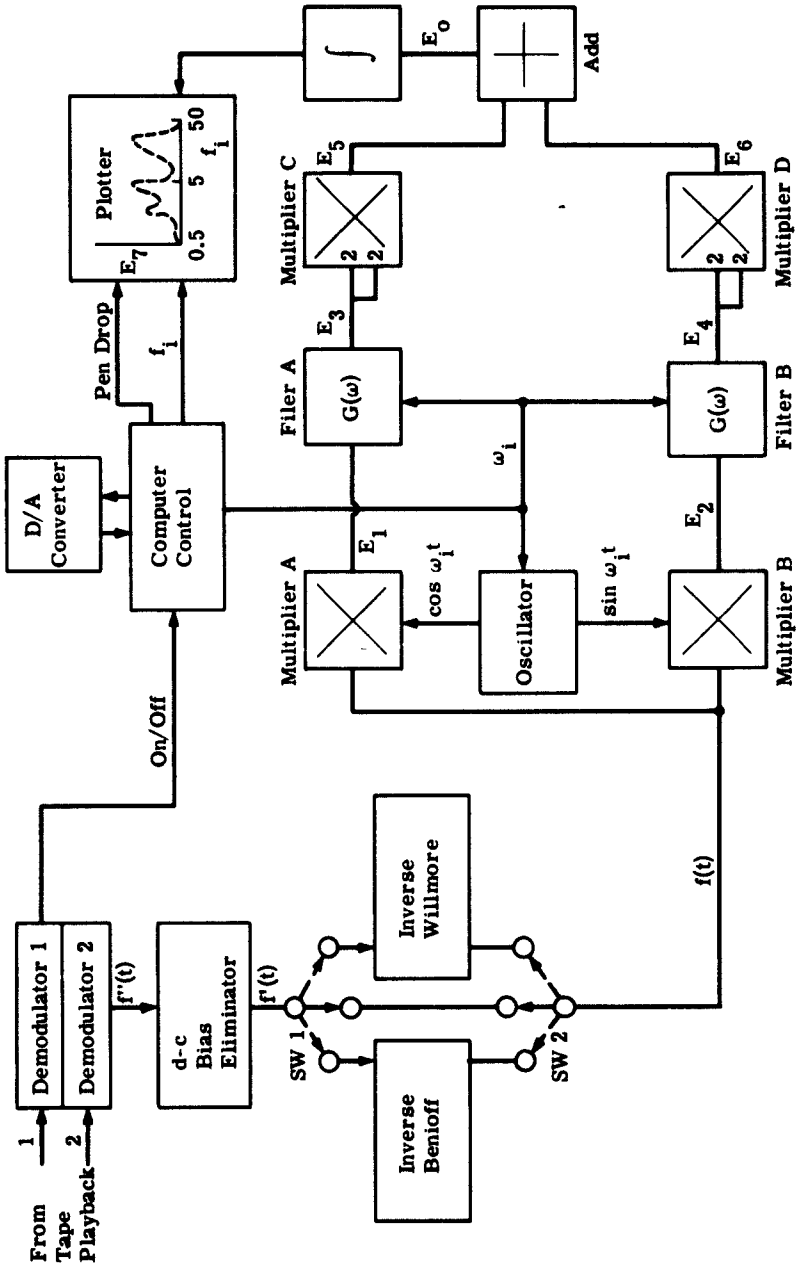

FIGURE 23. BLOCK DIAGRAM OF ANALOG COMPUTER USED FOR FREQUENCY ANALYSIS

The computer control block operates together with the digital-to-analog (D/A) converter to generate an analog voltage corresponding to a particular interrogation frequency ω_i for each computer run. This voltage operates servo-positioned potentiometers in the oscillator, in order to set it at the corresponding frequency, and in filters A and B so that the bandwidth of the filters will be proportional to the oscillator frequency. Multipliers C and D are servo multipliers used to square the outputs of filters A and B, respectively. By use of a gain of 2 at the multiplier inputs, the 1/2 is eliminated from the equation of the output of the filters; therefore the output of multiplier C becomes

$$E_5 = A^2 \sin^2 (\omega - \omega_i)t \; G^2(\omega - \omega_i)$$

for the upper channel and

$$E_6 = A^2 \cos^2 (\omega - \omega_i)t \; G^2(\omega - \omega_i)$$

for the lower channel.

The summing amplifier adds these two multiplier outputs (E_5) and (E_6) to produce at its output

$$E_o = E_5 + E_6 = A^2G^2(\omega - \omega_i)$$

This result is integrated to produce at the integrator output

$$E_7 = \int_0^T A^2G^2(\omega - \omega_i)\,dt$$

where T is the time of the seismic signal on the magnetic tape, or more precisely, the time of the "On" signal in the control channel.

The oscillating term has disappeared in the equation for the output of the adder:

$$E_o = A^2G^2(\omega - \omega_i)$$

However, it should be pointed out that the difference frequency ($\omega - \omega_i$) determines the filter response $G(\omega - \omega_i)$, and thus determines the attenuation of A, whereas interrogation frequency (ω_i) controls the bandwidth of the filter.

The control channel in Figure 23 is operated by a positive or negative voltage from demodulator 1. The control signals were recorded on a separate channel of the magnetic tape which contained the seismic signal to be analyzed. A positive voltage, or "On" signal, was recorded for the duration of the seismic signal. A negative voltage, or "Off" signal, was then recorded for about fifteen seconds after terminating the seismic signal. This magnetic tape was spliced into an endless loop which could be played continuously.

The operating sequence of the computer control follows. During the playback of the seismic signal, the control-channel voltage keeps the computer on "Operate," and the seismic signal is investigated for frequency components in the neighborhood of the interrogation frequency ω_i, to which the oscillator is set. At the end of the seismic signal, the "On" voltage from the control channel changes to an "Off" voltage; this change is sensed by the computer control and causes it to operate a relay which in turn switches the computer to the "Hold" mode. This stops all integrators in the computing circuit and maintains all analog voltages at their values at the end of the run. The "Off" voltage in the control channel also causes the controller to start a timing integrator whose output is connected to various differential relays, so arranged and connected that the following sequence is followed.

After a time interval long enough for the servo-driven multipliers, resolvers, and plotter to come to rest, a relay operates, momentarily dropping the pen on the plotter, and thereby plotting the value of E_7 from the integrator. Next, the hold condition is momentarily removed from the digital-to-analog converter, and the paper tape advances, reading the next set of values (ω_{i+1} for the oscillator and the filters, and f_{i+1} for the plotting table). Next, the computer is placed in the "Reset" mode, which establishes all initial voltages required for the problem at time "zero". The computer is now ready to receive an "On" signal to start the next computation at the beginning of the next playback cycle of the tape loop.

The D/A converter reads from a punched-paper tape on command from the computer control, and feeds this information back to the computer control in the form of a d-c voltage. The plotter is an X-Y plotting table having an external pen-drop circuit. The X is positioned by a voltage proportional to the interrogation frequency (ω_i); the Y is positioned by the value of the voltage at the output of the integrator E_7 at the end of each integration. Thus a line drawn through these integration end points produces a curve showing energy versus frequency for the entire signal. More detailed descriptions of the individual blocks of Figure 23 follow.

B.1.1. THE OSCILLATOR. The oscillator, which generates $\sin \omega_i t$ and $\cos \omega_i t$, is basically a three-amplifier oscillator loop where two of the amplifiers are integrators. This arrangement is shown schematically in Figure 24.

B.1.2. THE ELECTRONIC MULTIPLIER. Multipliers A and B of Figure 23 were actually two channels of a single electronic multiplier. This is a four-quadrant multiplier in that any combination of mathematical signs of input variables will always produce the correct sign on the output. The bandwidth of this multiplier is over 100 cps.

B.1.3. THE LOW-PASS FILTER. Filters A and B of Figure 23 were simple first-order low-pass units assembled from analog components, as shown in Figure 25.

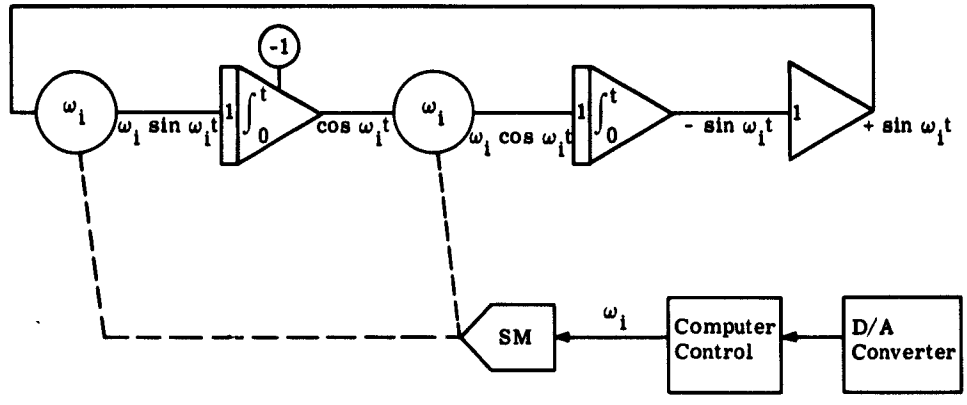

FIGURE 24. ANALOG-COMPUTER OSCILLATOR FOR GENERATING $\sin \omega_i t$ AND $\cos \omega_i t$

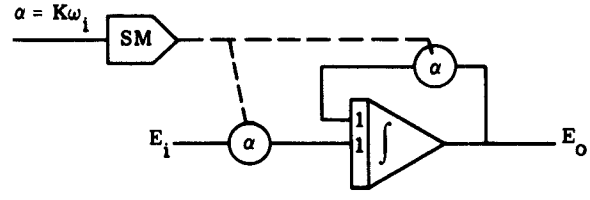

FIGURE 25. ANALOG-COMPUTER SCHEMATIC OF A LOW-PASS FILTER

If the integrator output is E_o, its input is $-E_o$, and the circuit solves the equation

$$\dot{E}_o + \alpha E_o = -\alpha E_i \tag{80}$$

Obtaining the Laplace transform of both sides of Equation 80 and assuming that $E_o(0)$ is zero,

$$sE_o(s) + \alpha E_o(s) = -\alpha E_i(s) \tag{128}$$

and solving for $\frac{E_o(s)}{E_i(s)}$

$$\frac{E_o(s)}{E_i(s)} = -\frac{\alpha}{s+\alpha} = -\frac{1}{1+s\tau} \tag{129}$$

where $\tau = 1/\alpha$.

If the filter circuit shown in Figure 25 is to have unity d-c gain, it is important that the potentiometer labeled (α) in the feedback path of the integrator have exactly the same setting as the (α) potentiometer in the input circuit. As with the previously described oscillator, these potentiometers are set by a servo multiplier so that the value of α is a function of the interrogation frequency $\omega_i/2\pi$. Any mismatch between these two potentiometers will affect the d-c gain of the filter and cause an apparent error in the filter response.

Figure 26 shows a rearrangement of the filter so that E_o and E_i are summed before multiplying by α instead of multiplying each by α and then summing at the input of the integrator. This arrangement insures a gain of unity.

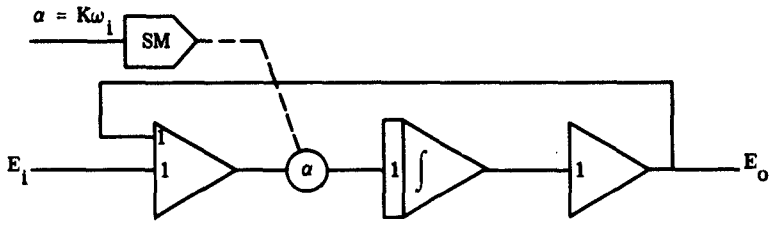

FIGURE 26. ANALOG-COMPUTER SCHEMATIC OF A LOW-PASS FILTER USING ONLY ONE (α) POTENTIOMETER

B.1.4. THE SQUARING MULTIPLIER. Multipliers C and D in Figure 23 were high-speed servo units used for squaring the signals from filters A and B, respectively, before they were added. Although electronic multipliers or function generators could have been used for this purpose, the servo multipliers were used because they were readily available and their speed was compatible with the frequency spectra of the signals coming from the low-pass filters.

A diagram of the squaring circuit is shown in Figure 27. The output of this circuit is always positive, regardless of the polarity of the input.

One particular advantage of the use of a servo multiplier for performing the squaring function is the lack of any residual output voltage when the input is zero. When diode function generators were used for squaring, considerable difficulty was encountered in reducing the drift resulting from output voltages produced by the function generators at zero input.

B.1.5. THE COMPUTER CONTROL AND DIGITAL-TO-ANALOG (D/A) CONVERTER. The computer control circuits are shown in Figure 28. When an off signal or minus voltage is received from the control channel, a switching amplifier (labeled "H.G." in Figure 28) switches the computer to the "Hold" mode of operation,

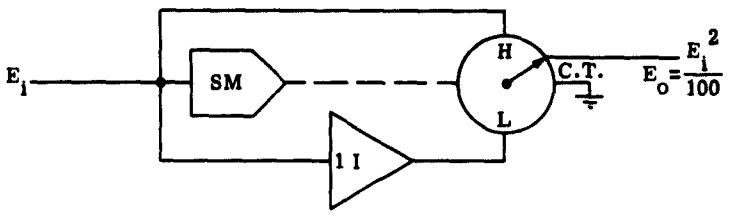

FIGURE 27. SERVO MULTIPLIER USED FOR SQUARING

thus retaining all voltages present at this point of the computation. The operation of a switching amplifier such as this is based on the action of a high-gain amplifier with two different diode-feedback circuits. When the input voltage E_i is positive, the output voltage E_o tends to be negative, but the diode L_1 produces a feedback path of approximately zero impedance; hence $E_o \approx 0$ and sensitive relay SK_1 is unenergized as shown. When E_i is positive, E_o tends to go positive and diode L_1 does not conduct. Under these circumstances, the feedback path must be through diode L_2. This feedback path is established for a positive E_o when the voltage at junction E_1 (between R_1 and R_2) is approximately zero. This action occurs only when $E_o \approx +100 \frac{R_1}{R_2}$. Thus, the output of the switching amplifier is either 0 or $+100 \frac{R_1}{R_2}$ volts, depending upon the polarity of the input voltage. With the proper ratio of R_1 to R_2, the minus "Off" voltage produces a plus E_o of sufficient amplitude to energize relay SK_1 and thereby switches the computer to the "Hold" mode. The RC-time-constant filter placed between the contacts of SK_1 and the hold relay reduces the off signal to a pulse and thus releases the hold command so that the computer can cycle.

The hold-command pulse, coming through network RC from the switching amplifier, also energizes relay K_1, and the "feedback" voltage from the computer hold circuits keeps K_1 energized. Relay K_1 switches voltage $\dot{t}$ into integrator 1 and removes the short-circuit from the integrator's feedback path, thus allowing the integration of $\dot{t}$. The voltage output (t) of integrator 1 rises, thereby supplying relays SK_2 and SK_3 with an increasing voltage. The most sensitive relay was chosen for SK_2; thus it operates first, produces a "pen-drop" signal through the RC network, and causes the X-Y plotter to produce a dot. Relay SK_3, operates next: it removes the "Hold" voltage from the D/A converter; allows it to read the next ω_i; and also puts the computer on the "Reset" mode, thus removing the computer Hold and de-energizing relay K_1. When the computer goes on "Reset," the integrator output t goes to zero, and, de-energizing SK_2 and SK_1, re-establishes the D/A hold and sets the computer for the "Operate" command.

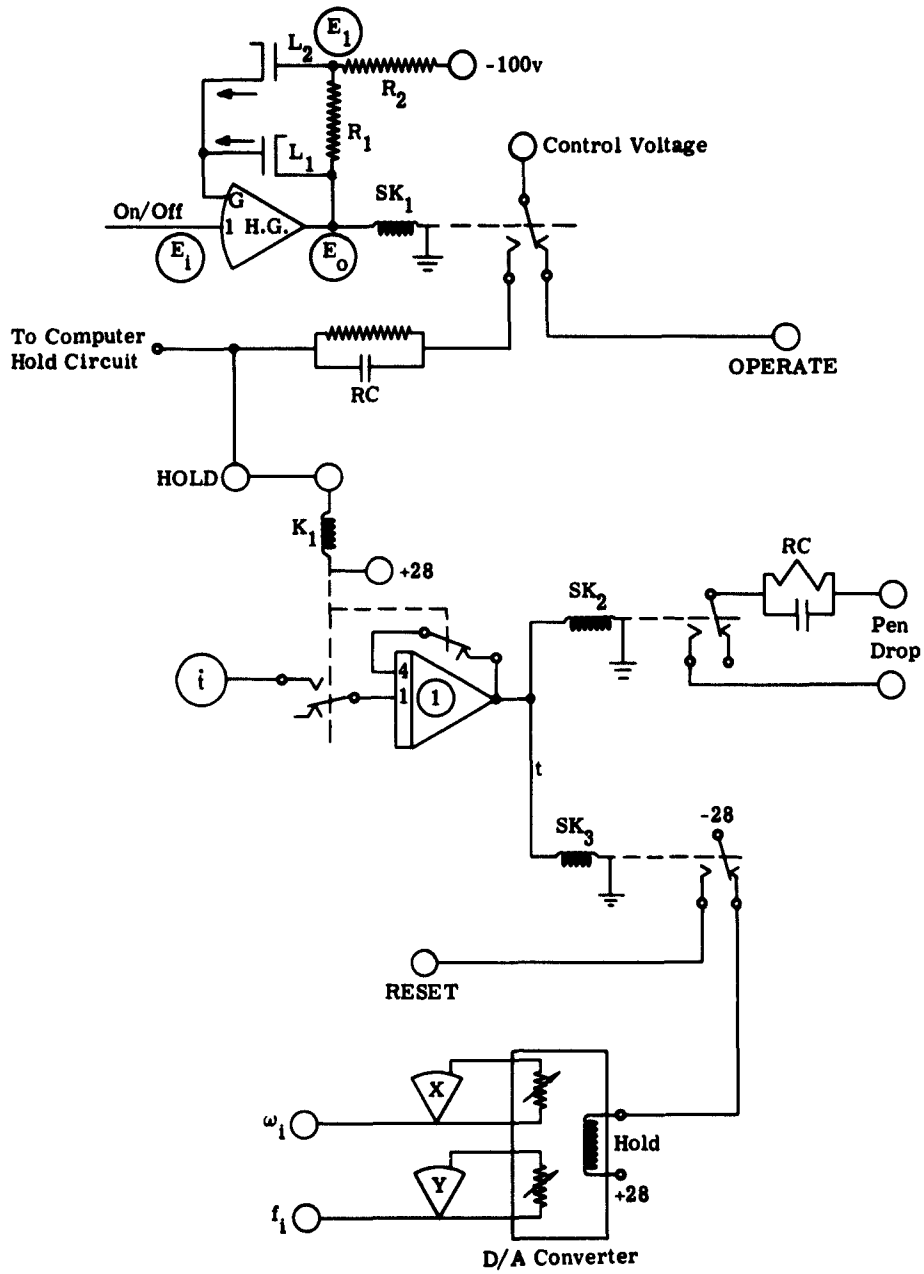

FIGURE 28. COMPUTER CONTROL AND D/A CONVERTER

REFERENCES

1. S. Goldman, Frequency Analysis, Modulation and Noise, McGraw-Hill, New York, N. Y., 1948, pp. 54-55.
2. Y. Lee, Statistical Theory of Communication, John Wiley & Sons, Inc., New York, N. Y., 1960, Chapter 2.
3. W. Davenport and W. Root, An Introduction to the Theory of Random Signals and Noise, McGraw-Hill, New York, N. Y., 1958, p. 107.
4. S. Goldman, Information Theory, Prentice-Hall, Inc., New York, N. Y., 1953, p. 244.
5. J. Otterman, "The Properties and Methods for Computation of Exponentially-Mapped Past Statistical Variables," IRE Trans. Auto. Control, January 1960, Vol. AC-5, No. 1, pp. 11-17.

DISTRIBUTION LIST

Copy No.	Addressee
1-15	Air Force Technical Applications Center Headquarters, USAF Washington 25, D. C. ATTN: TD-1
16-23	Headquarters, Air Force Office of Scientific Research Office of Aerospace Research, United States Air Force Washington 25, D. C.
(16-19)	ATTN: SRPG
(20)	ATTN: Commander SRG
(21-23)	ATTN: Commander SRGL
24-27	Advanced Research Projects Agency The Pentagon Washington 25, D. C.
28	RAND Corporation 1700 Main Street Santa Monica, California ATTN: Dr. R. Latter
29	California Institute of Technology, Seismological Laboratory Pasadena, California ATTN: Dr. F. Press
30	Continental Oil Company P. O. Drawer 1267 Ponca City, Oklahoma ATTN: Dr. J. Crawford
31	U. S. Coast & Geodetic Survey (Seismology Branch) Department of Commerce Washington 25, D. C.
32	National Science Foundation, Washington 25, D. C. ATTN: Earth Sciences Division
33	Naval Research Laboratory, Washington 25, D. C. ATTN: Librarian (Code 2027)
34-35	British Defense Research Staff, British Embassy 3100 Massachusetts Ave., N. W. Washington 8, D. C. ATTN: Atomic Coordinating Office
36	U. S. Geological Survey, Department of Interior Washington 25, D. C. ATTN: Crustal Studies
37-38	Institute for Defense Analysis, Universal Building Connecticut Ave., N. W. Washington 25, D. C. ATTN: RESD, Dr. J. M. Denoyer
39	Defense Atomic Support Agency The Pentagon Washington 25, D. C. ATTN: Blast & Shock Division
40	U. S. Army Research Office Box CM, Duke Station Durham, North Carolina
41	Bell Telephone Laboratory Murray Hill, New Jersey ATTN: Dr. B. Bogart
42	Office of Aerospace Research, Washington 25, D. C. ATTN: RROSG
43	U. S. Arms Control Disarmament Agency Department of State Washington 25, D. C. ATTN: Mr. D. Musser
44	Vela Data Analysis & Technique Development Center Headquarters, USAF Washington 25, D. C. ATTN: AFTAC/TD-1A
45-47	Air Force Cambridge Research Laboratory Hanscom Field Bedford, Massachusetts ATTN: SRZG
48	Seismological Laboratory, California Institute of Technology Pasadena, California ATTN: Dr. V. Hugo Benioff
49	Shell Development Company P. O. Box 481 Houston 1, Texas ATTN: Dr. Sidney Kaufman
50	Gulf Research & Development Company Box 2038 Pittsburgh 30, Pennsylvania ATTN: Dr. T. J. O'Donnell
51	Lamont Geological Observatory Palisades, New York ATTN: Dr. Jack E. Oliver
52	Institute of Technology, St. Louis University St. Louis, Missouri ATTN: Father Wm. V. Stauder, S.J.
53	Carnegie Institution of Washington Department of Terrestrial Magnetism 5241 Broadbranch Road, N. W. Washington, D. C. ATTN: Dr. John S. Steinhart
54	Director of Research & Development, Headquarters, USAF Washington 25, D. C. ATTN: AFDRD
55	Chief of Research & Development, Department of the Army Washington 25, D. C. ATTN: Scientific Information Branch
56	U. S. Atomic Energy Commission, Technical Information Extension P. O. Box 62 Oak Ridge, Tennessee
57	National Bureau of Standards Building 115 Washington 25, D. C. ATTN: Mr. Henry Matheson
58	Earth Sciences Division, National Science Foundation Washington 25, D. C. ATTN: Dr. R. Hanson
59	Air Force Systems Command Andrews Air Force Base Washington 25, D. C. ATTN: Commander SCRS
60	U. S. Bureau of Mines, Department of the Interior College Park Research Center College Park, Maryland ATTN: Mr. Wilbur I. Duvall
61	California Research Corporation P. O. Box 446 LaHabra, California ATTN: Dr. F. G. Blake, Jr.

DISTRIBUTION LIST (Continued)

Copy No.	Addressee
62	The Geotechnical Corporation P. O. Box 28277 Dallas 28, Texas ATTN: Mr. Jack Hamilton
63	Massachusetts Institute of Technology Cambridge 39, Massachusetts ATTN: Prof. Stephen M. Simpson
64	Pennsylvania State University, University Park, Pennsylvania ATTN: Prof. B. F. Howell, Jr.
65	Rensselaer Polytechnic Institute, Troy, New York ATTN: Dr. Samuel Katz
66	Sandia Corporation, Sandia Base Albuquerque, New Mexico ATTN: Dr. William R. Perret
67	Southern Methodist University, Dallas Seismological Observatory Dallas, Texas ATTN: Dr. Eugene Herrin
68	Stanford Research Institute, Menlo Park, California ATTN: Dr. Lawrence Swift
69	Texas Instruments, Inc. P. O. Box 35084 Dallas 35, Texas ATTN: Mr. T. T. Arnett
70	United ElectroDynamics, Inc. 200 Allendale Road Pasadena, California ATTN: Dr. E. A. Flinn
71	University of California, LaJolla Laboratories LaJolla, California ATTN: Dr. Walter Munk
72	University of California, Seismograph Station Berkeley, California ATTN: Prof. Perry Byerly
73	Texaco, Incorporated P. O. Box 425 Bellaire 101, Texas ATTN: Dr. Gerhard Herzog
74	Texaco, Incorporated P. O. Box 3109 Midland, Texas ATTN: Mr. F. H. Nicolai
75	University of Wisconsin, Geophysical & Polar Research Center 2544 University Avenue Madison 5, Wisconsin ATTN: Prof. R. P. Meyer
76	Sylvania Electronic Defense Laboratories P. O. Box 205 Mountain View, California ATTN: Arthur Bridgman
77	Analog Computing Facility, General Motors Technical Center Detroit, Michigan
78	United States Coast and Geodetic Survey, Field Laboratory Sandia Base, Albuquerque, New Mexico
79	United States Atomic Energy Commission Washington 25, D. C. ATTN: Major J. Rosen, DMA
80	Office of Naval Research Washington 25, D. C. ATTN: Code 410
81-90	Armed Services Technical Information Agency Arlington Hall Station Arlington 12, Virginia ATTN: TIPCR

AD Div. 2/10, 30/2

Inst. of Science and Technology, Univ. of Mich., Ann Arbor ANALOG COMPUTATION OF TIME-VARYING POWER SPECTRA OF SEISMIC WAVES by Vernon L. Larrowe and Raymond E. Crabtree. Apr. 63. 60 p., incl. illus., 5 refs. (Report No. 3708-15-T/5178-8-T) Unclassified Report (Contracts AF 49(638)-911, AF 49(638)-1170)

An analog computing technique for measuring time-varying power spectra of seismic signals has been developed. The signal to be analyzed is recorded on a magnetic-tape loop so that it may be played back repeatedly, and the analog computing equipment, connected to the output of the tape-playback apparatus, measures as a function of time the power level at a different specific frequency for each passage of the tape.

The concept of a time-varying spectrum is developed and the theory of the analysis method is derived. It is shown that in measuring time-varying power spectra, there is a theoretical relationship between the time resolution and frequency

(over)

UNCLASSIFIED

I. Larrowe, Vernon L., Crabtree, Raymond E.
II. U. S. Air Force
III. Contracts AF 49(638)-911 and AF 49(638)-1170

Armed Services Technical Information Agency
UNCLASSIFIED

AD Div. 2/10, 30/2

Inst. of Science and Technology, Univ. of Mich., Ann Arbor ANALOG COMPUTATION OF TIME-VARYING POWER SPECTRA OF SEISMIC WAVES by Vernon L. Larrowe and Raymond E. Crabtree. Apr. 63. 60 p., incl. illus., 5 refs. (Report No. 3708-15-T/5178-8-T) Unclassified Report (Contracts AF 49(638)-911, AF 49(638)-1170)

An analog computing technique for measuring time-varying power spectra of seismic signals has been developed. The signal to be analyzed is recorded on a magnetic-tape loop so that it may be played back repeatedly, and the analog computing equipment, connected to the output of the tape-playback apparatus, measures as a function of time the power level at a different specific frequency for each passage of the tape.

The concept of a time-varying spectrum is developed and the theory of the analysis method is derived. It is shown that in measuring time-varying power spectra, there is a theoretical relationship between the time resolution and frequency

(over)

UNCLASSIFIED

I. Larrowe, Vernon L., Crabtree, Raymond E.
II. U. S. Air Force
III. Contracts AF 49(638)-911 and AF 49(638)-1170

Armed Services Technical Information Agency
UNCLASSIFIED

AD Div. 2/10, 30/2

Inst. of Science and Technology, Univ. of Mich., Ann Arbor ANALOG COMPUTATION OF TIME-VARYING POWER SPECTRA OF SEISMIC WAVES by Vernon L. Larrowe and Raymond E. Crabtree. Apr. 63. 60 p., incl. illus., 5 refs. (Report No. 3708-15-T/5178-8-T) Unclassified Report (Contracts AF 49(638)-911, AF 49(638)-1170)

An analog computing technique for measuring time-varying power spectra of seismic signals has been developed. The signal to be analyzed is recorded on a magnetic-tape loop so that it may be played back repeatedly, and the analog computing equipment, connected to the output of the tape-playback apparatus, measures as a function of time the power level at a different specific frequency for each passage of the tape.

The concept of a time-varying spectrum is developed and the theory of the analysis method is derived. It is shown that in measuring time-varying power spectra, there is a theoretical relationship between the time resolution and frequency

(over)

UNCLASSIFIED

I. Larrowe, Vernon L., Crabtree, Raymond E.
II. U. S. Air Force
III. Contracts AF 49(638)-911 and AF 49(638)-1170

Armed Services Technical Information Agency
UNCLASSIFIED

AD Div. 2/10, 30/2

Inst. of Science and Technology, Univ. of Mich., Ann Arbor ANALOG COMPUTATION OF TIME-VARYING POWER SPECTRA OF SEISMIC WAVES by Vernon L. Larrowe and Raymond E. Crabtree. Apr. 63. 60 p., incl. illus., 5 refs. (Report No. 3708-15-T/5178-8-T) Unclassified Report (Contracts AF 49(638)-911, AF 49(638)-1170)

An analog computing technique for measuring time-varying power spectra of seismic signals has been developed. The signal to be analyzed is recorded on a magnetic-tape loop so that it may be played back repeatedly, and the analog computing equipment, connected to the output of the tape-playback apparatus, measures as a function of time the power level at a different specific frequency for each passage of the tape.

The concept of a time-varying spectrum is developed and the theory of the analysis method is derived. It is shown that in measuring time-varying power spectra, there is a theoretical relationship between the time resolution and frequency

(over)

UNCLASSIFIED

I. Larrowe, Vernon L., Crabtree, Raymond E.
II. U. S. Air Force
III. Contracts AF 49(638)-911 and AF 49(638)-1170

Armed Services Technical Information Agency
UNCLASSIFIED

AD

resolution such that any adjustment improving one degrades the other. This conflict is not due to equipment limitations, but instead is a result of theoretical relations between the time and frequency domains.

It is concluded that measuring methods based on the use of filters are theoretically equivalent to methods using weighted Fourier analysis, and that the choice of a method to be used should be based primarily upon equipment requirements. The analog-computer setup makes a very flexible tool for developing methods of power-spectra measurements, although more specialized apparatus would probably be more satisfactory after an optimum method has been found.

UNCLASSIFIED

DESCRIPTORS

Analog computer
Frequency analyzers
Seismic waves

UNCLASSIFIED

AD

resolution such that any adjustment improving one degrades the other. This conflict is not due to equipment limitations, but instead is a result of theoretical relations between the time and frequency domains.

It is concluded that measuring methods based on the use of filters are theoretically equivalent to methods using weighted Fourier analysis, and that the choice of a method to be used should be based primarily upon equipment requirements. The analog-computer setup makes a very flexible tool for developing methods of power-spectra measurements, although more specialized apparatus would probably be more satisfactory after an optimum method has been found.

UNCLASSIFIED

DESCRIPTORS

Analog computer
Frequency analyzers
Seismic waves

UNCLASSIFIED

AD

resolution such that any adjustment improving one degrades the other. This conflict is not due to equipment limitations, but instead is a result of theoretical relations between the time and frequency domains.

It is concluded that measuring methods based on the use of filters are theoretically equivalent to methods using weighted Fourier analysis, and that the choice of a method to be used should be based primarily upon equipment requirements. The analog-computer setup makes a very flexible tool for developing methods of power-spectra measurements, although more specialized apparatus would probably be more satisfactory after an optimum method has been found.

UNCLASSIFIED

DESCRIPTORS

Analog computer
Frequency analyzers
Seismic waves

UNCLASSIFIED

AD

resolution such that any adjustment improving one degrades the other. This conflict is not due to equipment limitations, but instead is a result of theoretical relations between the time and frequency domains.

It is concluded that measuring methods based on the use of filters are theoretically equivalent to methods using weighted Fourier analysis, and that the choice of a method to be used should be based primarily upon equipment requirements. The analog-computer setup makes a very flexible tool for developing methods of power-spectra measurements, although more specialized apparatus would probably be more satisfactory after an optimum method has been found.

UNCLASSIFIED

DESCRIPTORS

Analog computer
Frequency analyzers
Seismic waves

UNCLASSIFIED